Aus dem Department für Kleintiere und Pferde

der Veterinärmedizinischen Universität Wien

Klinik für Pferdechirurgie

Leitung: Prof.in Dr.in med. vet. Florien Jenner, Dipl. ACVS Dipl. ECVS

Development of an In Vitro Model for Inducing Cellular Senescence in Ovine Chondrocytes and Synoviocytes: Implications for Osteoarthritis Research

Diplomarbeit

Veterinärmedizinische Universität Wien

vorgelegt von

Anna Spielhofer

Wien, am 28.02.2024

Die vorliegende Diplomarbeit wurde in der Klinik für Pferdechirurgie - Arbeitsgruppe VETERM - unter Anleitung von Priv.-Doz. Dr.in med. vet Iris Gerner, PhD und Prof.in Dr.in med. vet. Florien Jenner, Dipl. ACVS Dipl. ECVS ausgeführt.

Begutachterin: Univ.-Prof.in Dr.in.med.vet. Jessika-Maximiliane Cavalleri, Dipl. ECEIM

Eigenständigkeitserklärung

Ich erkläre hiermit, dass ich die vorliegende Diplomarbeit selbstständig unter Anleitung verfasst und keine anderen als die angegebenen Quellen und Hilfsmittel benutzt habe.

Spielhofer

28.02.2024 Wien

Abstract

Osteoarthritis (OA) is a degenerative joint disease characterised by the presence of senescent cells. Chondrocytes and synoviocytes are the predominant cell types in the joint and play a critical role in the chronic progression of OA when they enter a state of senescence. It is thought that chronic inflammation, triggered by various factors such as genetics or joint injury, disrupts the cellular homeostasis of these cells, causing them to undergo cellular stress. Stress-induced cellular damage, particularly under conditions of homeostatic imbalance such as oxygen deprivation, can lead to cellular dysfunction, potentially pushing cells into senescence. Once cells enter senescence, they remain in a state of growth arrest for an indefinite period of time. Senescent cells produce Senescence-Associated Secretory Phenotype (SASP) factors, including pro-inflammatory cytokines such as IL-6 and IL-8, which contribute to cartilage degeneration. This in turn leads to a cascade of more chondrocytes and synoviocytes entering senescence due to the increased stress environment around the lesion caused by OA. Understanding the senescent state of chondrocytes and synoviocytes is critical to intervene and interrupt this cycle.

The aim of this study was to chemically induce senescence in chondrocytes and synoviocytes using Dexamethasone (at 20 μM, 10 μM, 5 μM and 1 μM) and Doxorubicin (at 200 nM, 100 nM, 50 nM and 25 nM) and to optimise the senescence induction protocol. Both drugs were tested using various assays and tests to allow dose titration and direct comparison. The results showed that Dexamethasone had no toxic effects on cells at any of the concentrations tested, as indicated by the MTT viability assay. A minimum of 72 hours incubation with Dexamethasone at all concentrations (20 μM, 10 μM, 5 μM, and 1 μM) was required to effectively upregulate senescence-associated gene expressions in chondrocytes, and 6 days incubation was the best duration. In chondrocytes, 1 μM Dexamethasone showed the highest up-regulation of senescence-associated genes, which was confirmed by the 3-day and 6-day titration assays. For synoviocytes, 5 μM Dexamethasone was identified as the optimal concentration.

Doxorubicin was cytotoxic at 200 nM and 100 nM was cytotoxic with reduced cell viability. Doxorubicin induced the highest expression of senescence-associated genes in both chondrocytes and synoviocytes at a concentration of 200 nM. To overcome this, a concentration of 50 nM was identified as non-toxic but still capable of inducing gene expression changes indicative of senescence.

In conclusion, the study provides insight into the optimal conditions and chemical agents for inducing senescence in chondrocytes and synoviocytes. These findings lay the groundwork

for future studies aimed at reversing senescence and developing potential treatments for OA. It should be noted that although our in vitro results shed light on the senescent state, they may not fully reflect the in vivo conditions of OA. Further investigations, such as beta-galactosidase assays and cytokine analysis, are recommended to further our understanding of the senescent state.

Zusammenfassung

Osteoarthritis (OA) ist eine degenerative Gelenkerkrankung, die durch das Vorhandensein von alternden Zellen gekennzeichnet ist. Chondrozyten und Synoviozyten sind die vorherrschenden Zelltypen im Gelenk und spielen eine entscheidende Rolle beim chronischen Fortschreiten der OA, wenn sie in einen Zustand der Seneszenz eintreten. Es wird angenommen, dass chronische Entzündungen, die durch verschiedene Faktoren wie Genetik oder Gelenkverletzungen ausgelöst werden, die zelluläre Homöostase dieser Zellen stören und sie in einen zellulären Stresszustand versetzen. Stressbedingte Zellschäden, insbesondere unter Bedingungen eines homöostatischen Ungleichgewichts wie Sauerstoffmangel, können zu zellulärer Dysfunktion führen und die Zellen möglicherweise in die Seneszenz treiben. Sobald Zellen in die Seneszenz eintreten, verbleiben sie für unbestimmte Zeit in einem Zustand des Wachstumsstillstands. Seneszente Zellen produzieren SASP-Faktoren (Senescence-Associated Secretory Phenotype), darunter entzündungsfördernde Zytokine wie IL-6 und IL-8, die zur Degeneration des Knorpels beitragen. Dies wiederum führt zu einer Kaskade von mehr Chondrozyten und Synoviozyten, die aufgrund der durch die OA verursachten erhöhten Stressumgebung um die Läsion in die Seneszenz eintreten. Das Verständnis des seneszenten Zustands von Chondrozyten und Synoviozyten ist entscheidend, um in diesen Zyklus einzugreifen und ihn zu unterbrechen.

Ziel dieser Studie war es, die Seneszenz in Chondrozyten und Synoviozyten mit Hilfe von Dexamethason (20 µM, 10 µM, 5 µM und 1 µM) und Doxorubicin (200 nM, 100 nM, 50 nM und 25 nM) chemisch zu induzieren und das Seneszenzinduktionsprotokoll zu optimieren. Beide Medikamente wurden mit verschiedenen Assays und Tests getestet, um eine Dosistitration und einen direkten Vergleich zu ermöglichen. Die Ergebnisse zeigten, dass Dexamethason bei keiner der getesteten Konzentrationen toxische Auswirkungen auf die Zellen hatte, wie der MTT-Lebensfähigkeitstest zeigte. Eine mindestens 72-stündige Inkubation mit Dexamethason in allen Konzentrationen (20 µM, 10 µM, 5 µM und 1 µM) war erforderlich, um die Seneszenz-assoziierten Genexpressionen in Chondrozyten wirksam hochzuregulieren, und eine Inkubation von 6 Tagen war die beste Dauer. In Chondrozyten zeigte 1 µM Dexamethason die stärkste Hochregulierung von Seneszenz-assoziierten Genen, was durch die 3-tägigen und 6-tägigen Titrationsversuche bestätigt wurde. Für Synoviozyten wurde 5 µM Dexamethason als optimale Konzentration ermittelt.

Doxorubicin war bei 200 nM zytotoxisch und 100 nM waren zytotoxisch, wobei die Lebensfähigkeit der Zellen deutlich reduziert war. Doxorubicin induzierte die höchste Expression von seneszenzassoziierten Genen sowohl in Chondrozyten als auch in

Synoviozyten bei einer Konzentration von 200 nM. Allerdings zeigte der MTT-Test, dass die Konzentrationen von 200 nM und 100 nM Doxorubicin toxisch waren und zum Zelltod führten. Um dies zu vermeiden, wurde eine Konzentration von 50 nM als nicht toxisch identifiziert, die aber immer noch in der Lage ist, Veränderungen in der Genexpression auszulösen, die auf Seneszenz hindeuten.

Zusammenfassend lässt sich sagen, dass die Studie einen Einblick in die optimalen Bedingungen und chemischen Wirkstoffe für die Auslösung von Seneszenz in Chondrozyten und Synoviozyten gibt. Diese Ergebnisse bilden die Grundlage für künftige Studien, die darauf abzielen, die Seneszenz umzukehren und potenzielle Behandlungen für OA zu entwickeln. Es sei darauf hingewiesen, dass unsere In-vitro-Ergebnisse zwar Aufschluss über den seneszenten Zustand geben, aber möglicherweise nicht vollständig die In-vivo-Bedingungen der OA widerspiegeln. Weitere Untersuchungen, wie z. B. Beta-Galaktosidase-Assays und Zytokinanalysen, werden empfohlen, um unser Verständnis des seneszenten Zustands zu vertiefen.

Table of Content

1. Introduction

1.1. Structure of a Joint

Joints are the movable points of contact between two bony or cartilaginous skeletal elements. Three types of joints are distinguished: fibrous joints, cartilaginous joints, and synovial joints. Here, we focus on synovial joints, known as "true joints," characterized by a joint cavity. Synovial joints consist of the following basic structures: articular surfaces, articular cartilage, joint capsule, joint cavity, synovial fluid, ligaments, and several intra-articular structures for example, articular menisci serve to compensate incongruities in the joint, articular labra enhance load-bearing capacity, and intraarticular ligaments fulfill a mechanical function (1–3).

1.1.1. Articular cartilage

Hyaline articular cartilage has a smooth surface that allows for frictionless and shock-absorbing movement of the joint, providing resistance to pressure (4). The cartilage thickness depends on the anatomical location, ranging from 1,5 millimetres to 2 millimetres (5). The articular cartilage is composed of approximately 1-12% chondrocytes and the extracellular matrix (ECM). The ECM consists of 75% water, 15% type 2 collagen, and 10% proteoglycans. It lacks nerves, blood vessels and lymphatics. The cartilage is nourished by synovial fluid produced by synoviocytes. It has a complex microstructure divided into four zones based on the shape of chondrocytes, the arrangement of collagen fibers, and the composition of the ground substance.

The nearest layer to the joint space, constituting 10-20% of the cartilage, is the tangential fiber zone (superficial zone). It contains the apices of collagen fibres running deep into the cartilage. Chondrocytes are spindle-shaped and oriented parallel to the surface. The water-binding capacity is highest in this layer, and age-related changes are most prominent here.

Next is the transitional zone (intermediate zone) constituting 40-60% of the cartilage, characterized by the arches formed by obliquely organized collagen fibres and spherically shaped chondrocytes.

Subsequently, the radial zone (deep zone) constituting around 30% of the cartilage, follows, where collagen fibers run perpendicular to the joint surface. Chondrocytes are arranged in a columnar manner and contain abundant endoplasmic reticulum.

The zone adjacent to the bone is referred to as the mineralization zone (subchondral bone lamina). Its function is to transmit pressure from the articular cartilage to the underlying bony joint ends. Few chondrocytes are present in this zone. During the growth phase, endochondral ossification occurs in this zone (2, 1, 3, 6–9).

1.1.1.1. Chondrocytes

Chondrocytes are embedded in the layers of the extracellular matrix (ECM) in avascular articular cartilage, where low nutrient and oxygen levels prevail. (4) Although chondrocytes are glycolysis-dependent, they require oxygen for some metabolic functions. Oxygen is supplied to them by the synovial fluid. Healthy chondrocytes have a robust defence mechanism against nitric oxide, free radicals, and reactive oxygen species (ROS). This defence mechanism is highly dependent on inflammatory mediators and the availability of oxygen within the cell (10). Chondrocytes form the basis of cartilage tissue function and matrix maintenance, which involves anabolic-catabolic balance (11). They actively proliferate and generate a variety of chondrocytes that differentiate slightly based on the needs of their microenvironment (12).

1.1.1.2. Synoviocytes

Synoviocytes are found in the thin inner layer of the joint capsule, forming a layer called the stratum synoviale that attaches to the edge of the articular cartilage. Two types of synoviocytes are distinguished: A-synoviocytes (“macrophagic” cells), which belong to the phagocytic system, and B-synoviocytes (fibroblast-like cells), which are similar to fibroblasts (13, 14).

Type A synoviocytes originate from blood-borne mononuclear cells and can be referred to as synovial tissue macrophages. However, they differ from other macrophages as they exhibit microvilli and microplicae on their surface, features not present in ordinary macrophages. They are immunoreactive to monoclonal antibodies against macrophages and express major histocompatibility class II molecules and antigens from the cluster differentation groupe 1a, playing a role in antigen presentation during the early immune response. During inflammatory processes, many macrophagic cells migrate from the blood to the synovial intima. They perform tasks such as absorbing extracellular “waste” material like extracellular matrix debrit, cell fragments, and antigens in the synovial fluid and intimal matrix. It is assumed that Type A cells, capable of absorbing numerous proteins, can modify them, thereby altering the protein composition of the synovial fluid. They are mainly located in the most superficial layer.

On the other hand, Type B cells are found further from the joint lumen, forming a thicker layer. Characterized by abundant rough endoplasmic reticulum, indicating active protein synthesis, and dendritic processes forming a network in the joint wall-facing side of the synovial membrane. Type B synoviocytes exhibit diverse shapes and extensions during cytoplasmic development. They resemble smooth muscle cells or myofibroblasts, as their cytoplasma includes many actin filaments and caveola systems. Type B cells are involved in the production

of specific products such as hyaluronan, collagens, and fibronectin, essential for the intimal interstitium and synovial fluid.

Notably, the proliferation rate of Type B cells is much higher than of Type A cells (14).

1.2. Osteoarthritis

Osteoarthritis is a painful and debilitating disease of the synovial joint (15). It is characterized by progressive degenerative changes in the morphology, composition, and mechanical properties of articular cartilage, synovium, and other components of the joint (16). Under normal circumstances, chondrocytes maintain homeostasis, which relies on a constant slow turnover of the cartilage extracellular matrix (ECM). This metabolic balance is disrupted in osteoarthritis. The underlying causes can be genetic, environmental (involving soluble mediators or local matrix composition), or biophysical (involving mechanical or osmotic stress) (15).

For a long time, osteoarthritis was considered a "wear and tear" condition, solely caused by aging and damage to the cartilage (17, 6). However, inflammation also plays a crucial role, as the treatment of osteoarthritis has shifted to target not only the injury but also the inflammation. It has been recognized that cytokines and immune cells play an important role in the pathology of osteoarthritis (15, 18, 19). Chondrocytes stimulated by pro-inflammatory cytokines, in particular, produce a large amount of nitric oxide, which is a hallmark of osteoarthritis and responsible for inhibiting the production of cartilage ECM with the help of important autocrine and paracrine factors (11). Additionally, there is activation of the innate immune system, which is involved in chronic inflammation (17).

Currently, there are no disease-modifying therapies for osteoarthritis. To regulate the abnormal cell behaviour in the joints affected by osteoarthritis, new therapeutic targets need to be discovered (20).

1.3. Senescence

Senescence is a state in which cells undergo a permanent halt in their cell cycle in response to various types of harmful stimuli (21). Instead of continuing to divide, these cells enter a state of prolonged dormancy. This occurs as a protective mechanism in response to factors such as DNA damage, oxidative stress, or the activation of oncogenes (22). Rather than undergoing programmed cell death (apoptosis), senescent cells remain metabolically active but are no longer capable of dividing. They also exhibit changes in gene expression and secrete a range of factors known as the senescence-associated secretory phenotype (SASP), which can have both positive and negative effects on neighbouring cells and tissues. Senescence represents a complex cellular response that plays a role in various biological processes, including aging and age-related diseases (22).

1.3.1. Fundamental mechanism of Senescence

It was discovered that replicative senescence is caused by the shortening of telomeres, the protective ends of linear chromosomes. Telomere shortening occurs when DNA polymerase is no longer able to fully replicate the ends of chromosomes, leading to complete cessation of telomerase expression. While some cells like germ cells and specialized cells can prevent telomere erosion by the action of telomerase, fibroblasts and many other differentiated cell types cannot (23). Cells exhibiting replicative senescence display a high heterogeneity in their division behaviour. In addition to telomere erosion, other detrimental conditions such as oxidative stress, DNA damage, radiation, or the expression of oncogenes can trigger cellular senescence (22, 23).

1.3.2. Types of Senescence

Due to the different methods of inducing senescence in vitro, various types of senescence have been identified. However, it is still unknown if all of these types occur in vivo (21).

1.3.2.1. Replicative Senescence (RS)

Replicative senescence refers to the loss of cell proliferation potential after multiple rounds of division, leading to cell cycle arrest (21). It is a response to chronic macromolecular damage. Cells halt mainly in the G2 phase of the cell cycle due to the gradual shortening of telomeres during replication, triggering the DNA damage response (DDR) at the G2/M transition to prevent proliferation of damaged cells (24).

Some cells can repair this damage allowing them to continue the cell cycle and proceed through mitosis. Two pathways are described for cells that still undergo mitosis but are brought to a halt in the cell cycle and enter cellular senescence.

On one hand the so called low chronic damage pathway, if DNA damage occurs again in the next G1 phase, the daughter cells immediately exit the cell cycle after mitosis (shown as the blue pathway in the Figure 1). They remain in a diploid state and do not further divide. On the other hand, persistent DNA damage signals resulting from severe DNA lesions lead to exit in the G2 phase. This results in the premature activation of APC/C CDH1 due to the accumulation of p21. As a consequence, these cells bypass mitosis, leading to chromosome duplication without subsequent cell division (tetraploidy) and entering a permanent G1 arrest (shown as the red pathway in the Figure) (23).

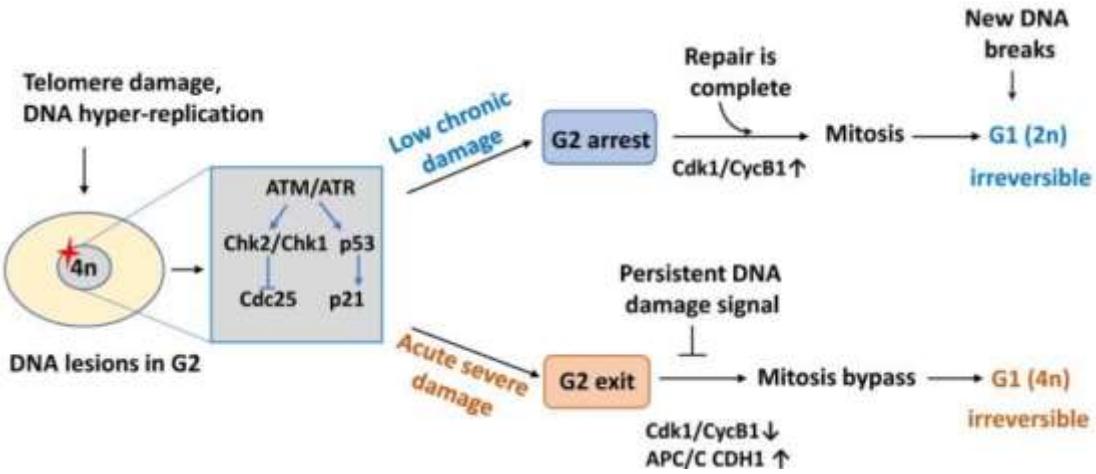

Figure 1 Schematic diagram of cell cycle arrest in senescence (Roger et al. 2021)

1.3.2.2. Stress-induced premature Senescence (SIPS)

Stress-induced premature senescence (SIPS) can be triggered by various factors that induce cellular stress, including oxidative stress, DNA damage, radiation-induced damage, or inflammatory stimuli (25). SIPS can be distinguished from replicative senescence in that telomere shortening is either not observed or is minimal in SIPS. Instead, it is believed that SIPS is initiated by random DNA damage occurring throughout the genome, followed by the activation of DNA damage response (DDR) pathways, which ultimately drive the cells into senescence. In SIPS, the telomeres are not shortened but rather damaged or compromised (26).

1.3.2.3. Oncogene-induced Senescence (OIS)

Oncogene-induced senescence is an anti-proliferative response triggered by oncogenic signals, which can result from the activation of an oncogene or the inactivation of tumour suppressor genes (27). Cells that undergo oncogene-induced senescence can still secrete oncogenic threats despite being in a senescent state (28).

1.3.2.4. Chemically-induced Senescence

Chemically induced senescence is triggered by many anticancer medications. These medications either cause DNA damage or disrupt the cell cycle through mechanisms such as inhibiting (CDKs) that control the cell cycle. In this study, the two substances Dexamethasone and Doxorubicin were used to induce chemically senescence in cells. The chapters on Dexamethasone and Doxorubicin provide further details on these substances and their effects on senescence (21).

It is important to note that these four forms of senescence, as described earlier, can overlap with each other. The specific type of senescence that a cell undergoes depends on the surrounding conditions and triggers to which the cells are exposed.
However, in this study, the focus is exclusively on replicative and chemical-induced senescence.

1.3.3. Senescence in Osteoarthritis

In a cartilage affected by osteoarthritis, many senescent chondrocytes can be found. However, it is still unclear how exactly these senescent cells contribute to osteoarthritis. Senescent synoviocytes have also been identified in the joints of individuals with osteoarthritis, and it has been observed that these cells promote osteoarthritic changes. Both senescent chondrocytes and synoviocytes produce senescence-associated secretory phenotype (SASP) factors. SASPs are responsible for promoting cartilage degeneration and subchondral bone remodeling in an inflammatory environment such as osteoarthritis, leading to the loss of cartilage tissue and worsening of the condition (19).

1.3.3.1. Senescence-associated secretory phenotype (SASP) factors

Senescent cells, despite being in a state of growth arrest, can produce and release a complex mixture of extracellular modulators like proinflammatory cytokines (for example IL-6, IL-8, IL-1beta and TNF alpha), chemokines, growth factors and protease known as the senescence-associated secretory phenotype (SASP). The composition of SASP varies depending on the cell type. SASP has both positive and negative functions. One of its main roles is to stimulate the immune system to eliminate senescent cells, involving both active and passive immune mechanisms. SASP also contributes to tissue remodeling in fibrotic tissues by releasing matrix metalloproteinases (MMPs for example MMP1 and MMP13) and other factors that initiate angiogenesis and reduce fibrosis. SASP facilitates communication between senescent cells and their surrounding environment (24).

Furthermore, the SASP is responsible for the paracrine senescence response, which is associated with persistent chronic inflammation, a key factor in osteoarthritis. This response includes factors such as IL-6, IL-8, monocyte chemoattractant proteins (MCPs), macrophage inflammatory proteins (MIPs), and other proteins involved in regulating various aspects of inflammation (29).

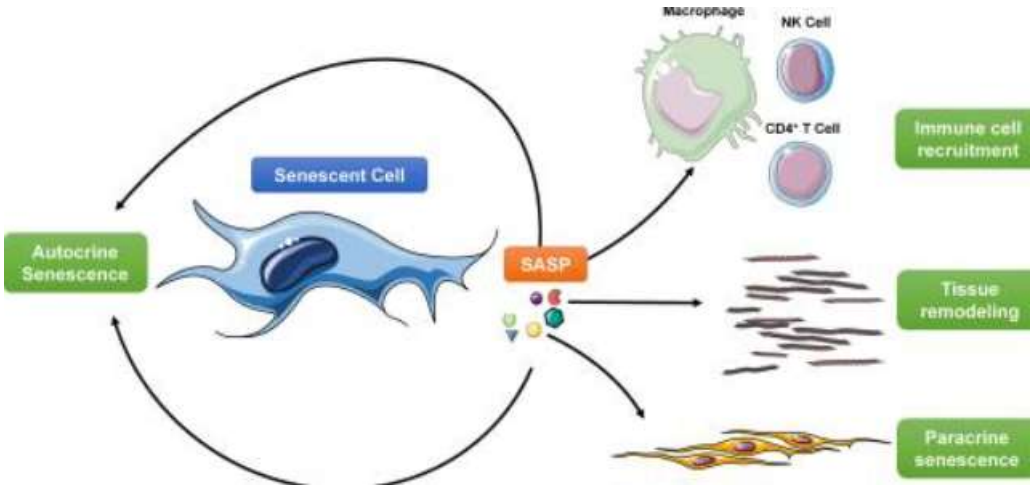

Figure 2 Functions of the SASP (McHugh and Gil 2018)

The SASP is positively regulated by the DNA damage response (DDR) and transcription factors such as nuclear factor NF-kB (Nuclear factor 'kappa-light-chain-enhancer' of activated B-cells) and C/EBP-β (CCAT/Enhancer Binding Protein). On the other hand, p53 plays a

negative regulatory role. Notably, C/EBP-β is essential for senescent cells and has been shown to be upregulated in oncogene-induced senescence, particularly in its binding to the IL-6 promoter (30). However, this study does not specifically focus on C/EBP-β as it pertains to oncogene-induced senescence which is not topic of this thesis.

1.3.3.2. Nuclear factor 'kappa-light-chain-enhancer' of activated B-cells (NF-κB)

NF-κB is a transcription factor that plays a central role in immune response, cell proliferation, and inflammatory responses. In osteoarthritis, NF-κB is involved in various processes, including chondrocyte catabolism, synovial inflammation, and chondrocyte survival. Therefore, the regulation, co-factors, and downstream effectors of NF-κB are of great importance.

When NF-κB translocates to the cell nucleus and binds to NF-κB response elements, it transactivates the expression of hundreds of different immunomodulatory proteins, pro-inflammatory cytokines, chemokines, adhesion molecules, and growth factors. In osteoarthritis, NF-κB induces the expression of matrix-degrading enzymes and other factors associated with the disease, either directly or indirectly, leading to an abnormal cartilage catabolic pathway (31). Not all pro-inflammatory genes expressed in senescent cells are dependent on NF-κB, but many are regulated by this master transcription factor (30).

1.3.3.3. DNA-damage-response (DDR) - ATM-p53-p12 pathway

The DNA damage response (DDR) is responsible for detecting DNA damage, transmitting information, and initiating repair processes (32, 23). (23)In the case of senescence, DDR is triggered by progressive telomere erosion, which leads to uncapped free double-stranded chromosome ends. Ataxia Telangiectasia Mutated (ATM), a damage sensor, is recruited to the damaged DNA site (33). ATM stabilizes the tumour suppressor protein p53 and upregulates p21, a transcriptional target of p53. P21 inhibits Cyclin-dependent Kinase 2 (CDK2) from inactivating Retinoblastoma protein (pRB), resulting in cell cycle arrest in the G1 or G2 phase and driving senescence. The growth arrest mediated by the p53/p21 pathway is believed to be reversible (34, 30). There is also a DDR-independent pathway involving P16INK4A-pRB, which interacts with other cyclin-dependent kinase inhibitors and leads to irreversible growth arrest (35, 30). (30) However, this pathway is not discussed in this study.

1.3.3.4. Reactive oxygen species (ROS)

The increase in reactive oxygen species (ROS) in cells leads to reduced autophagy, disrupting tissue homeostasis and contributing to the severity of osteoarthritis. The oxidative stress experienced by chondrocytes in osteoarthritis is associated with lower mitochondrial DNA content and mitochondrial mass, leading to mitochondrial dysfunction. This dysfunction results in reduced expression of SIRT1 (35).

1.3.3.4.1. Catalase

Catalase is one of the key antioxidant enzymes that counteracts oxidative stress in cells. It functions by breaking down cellular hydrogen peroxide into water and oxygen (36), (37). This process helps maintain an optimal level of molecules within the cell, which is crucial for healthy cellular signalling processes. Dysfunction or deficiency of catalase is believed to play a significant role in degenerative diseases such as osteoarthritis (38).

1.3.3.5. Hallmarks of Cellular Senescence

Senescence-associated β-galactosidase (SA-β-gal) and p16 were initially identified as markers for senescence and have been used to identify senescent cells. The arrest of the cell cycle is also associated with increased levels of cell cycle inhibitors such as p16INK4a, p21CIP1, and p27. Additionally, senescent cells exhibit higher expression of other biomarkers including p19ARF, p53, and PAI-1 as well (39). It has been shown that the expression of these markers increases with age in vivo. Currently, there is no single marker that can definitively detect senescent cells. Therefore, a combination of multiple markers is commonly used to identify senescent cells (22).

In the subsequent chapters, the biomarkers that were investigated in the course of the experiments for this study will be discussed in detail.

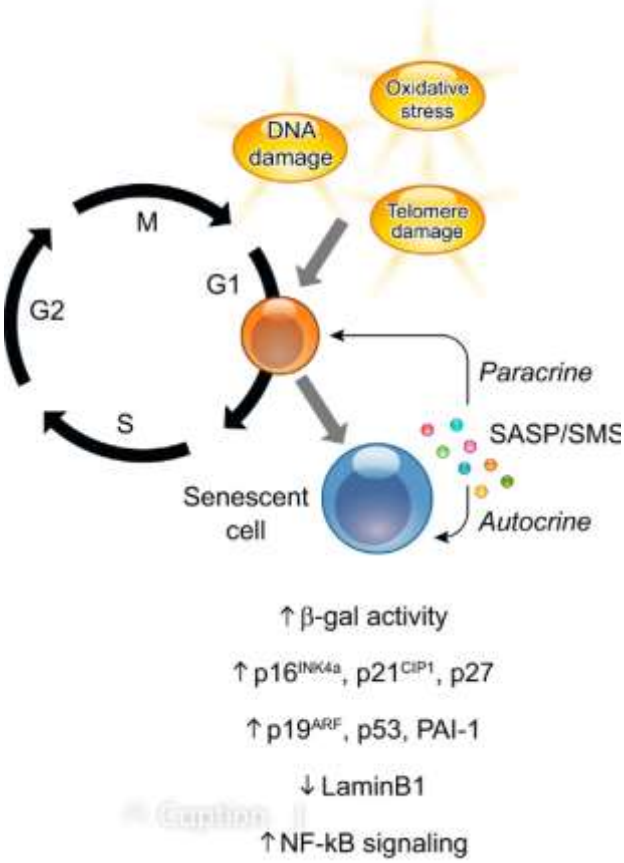

Figure 3 Characteristics of cellular senescence (Calcinotto et al. 2019)

1.3.3.5.1. senescence-associated β-galactosidase (SA-β-gal)

Senescent cells are known to exhibit increased activity of the enzyme senescence-associated β-galactosidase (SA-β-gal). SA-β-gal activity can be measured using flow cytometry with fluorescein di-D-galactopyranoside, which is cleaved by senescence-associated β-galactosidase. This process is referred to as SA-β-gal staining (40).

In healthy cells, the upregulation of SA-β-gal activity is best detected at a pH of 4, while in senescent cells, the optimal range is around pH 6. However, several factors need to be considered when using SA-β-gal as a marker for senescent cells in the joint. SA-β-gal staining in cultured chondrocytes may reflect an increase in autophagy rather than entry into a senescent state, as the enzymatic activity of lysosomes is regulated by the autophagy pathway. Additionally, a multiplication of lysosomes during cell growth, beta-galactosidase levels can also increase.

It is important to note that there are cases where SA-β-gal staining may not be present in senescent cells, such as in certain genetic disorders or when lysosomal function is impaired. Therefore, relying solely on SA-β-gal staining may not be sufficient for the detection of senescent cells. Other senescence markers and additional assays should be considered to complement SA-β-gal staining in the identification of senescent cells (41).

1.3.3.5.2. P53

P53 is a tumour suppressor protein, and such proteins have the ability to regulate and suppress the expression of proteins that activate cell cycle steps (42). Specifically, p53 plays a role in apoptosis and negatively regulates the SASP. P53 is activated in response to DNA damage caused by stress, earning it the title of a stress-responsive transcription factor (43). Normally, p53 is downregulated, but when there is DNA damage, increased production of p53 occurs, leading to its phosphorylation and stabilization and activation by ATM (refer to the corresponding chapter) (44, 45). Subsequently, p53 activation leads to a cell cycle arrest, facilitated by effectors such as p21 or endogenous cyclin-dependent kinase (CDK) inhibitor (43, 42).

1.3.3.5.3. P21

P21 is a protein involved in cell cycle regulation and the inhibition of multiple cell cycle-regulating cyclin-dependent kinases (CDKs). Various stimuli induce upregulation of p21, primarily through p53's transactivation. P21, as a single marker for senescence, is insufficient as it can be activated by various microRNAs or RNA-binding proteins independently of p53 (21).

1.3.3.5.4. LaminB1

LaminB1 is a widely used marker to detect senescence as its expression is downregulated in senescent cells. It is translocated to the cell nucleus and degraded by lysosomes. The downregulation of LaminB1 is dependent on p53 and other senescence-associated signalling pathways (21).

1.3.3.5.5. SIRT1

Sirtuins are a type of proteins that function as NAD+-dependent histone deacetylases. They are enzymes that can modify histones, thereby indirectly influencing the expression of certain

genes (35). They play a role in DNA repair, metabolism, stress response, cellular homeostasis, and aging (46).

In the context of cartilage tissue, SIRT1 has been most extensively studied. When SIRT1 is eliminated, it has been shown to lead to a faster progression of osteoarthritis, as well as increased susceptibility of the cartilage tissue to aging processes and mechanical stress. Under proinflammatory stress, which is characteristic of chronic osteoarthritis, SIRT1 is cleaved in chondrocytes. This results in the formation of an inactive N-terminal (NT) polypeptide and a C-terminal (CT) fragment, which are used as indicators in the serum to detect early osteoarthritis and chondrosenescence. Additionally, SIRT1, along with the cartilage-specific transcription factor Sox9, promotes the transcription of collagen 2, which forms the fibres in cartilage (19).

1.3.3.5.6. Telomerase reverse transcriptase (TERT)

At the ends of linear chromosomes, there are telomeres regulated by specialized enzymes called telomerases (47). Telomerase Reverse Transcriptase (TERT) plays a crucial role in telomere length and cell proliferation (48). TERT is responsible for telomere shortening, and telomere shortening indicates replicative senescence. (49) Most cells exhibit minimal TERT activity. Activation of TERT is often mediated by the NF-kB signalling pathway (47).

1.3.4. Chemical introduction of Senescence in Chondrocytes and Synoviocytes in vitro

1.3.4.1.1. Dexamethasone

Dexamethasone is a synthetic corticosteroid hormone widely used as a medication for inflammation, allergyies, immunsupression, cancer and for the treatment of respiratory or skin conditions. Its effects are anti-inflammatory and immune-suppressing (24, 50). It is used to reduce pain caused by osteoarthritis. Dexamethasone disrupts chondrocytes' metabolic balance toward catabolism, increases matrix metalloproteinase production, inhibits cell autophagy and thus can accelerate chondrocyte senescence, apoptosis, and death (24, 51). Prolonged treatment with Dexamethasone intensifies this effect (24, 51, 24, 52).

1.3.4.1.2. Doxorubicin

Doxorubicin is widely used in chemotherapy, although its exact mechanism of action is not fully understood. During chemotherapy, it often affects non-target tissues, which has a negative impact on the health of the patients (53). Doxorubicin induces senescence, as evidenced by the upregulation of p21 and p53 in cells treated with Doxorubicin, indicating senescence. However, prolonged treatment with Doxorubicin has been shown to increase apoptotic cell death (54). In chondrocytes, Doxorubicin suppresses cell differentiation by stimulating ROS production, leading to mitochondrial dysfunction, which can trigger senescence. Moreover, Doxorubicin induces DNA damage by causing DNA strand breaks and inhibiting the activity of topoisomerases, which play a crucial role in DNA replication and can also contribute to cell senescence (55, 56). Cells treated with Doxorubicin also showed activation of DDR and NF-kB, both are known to play a role in senescent cells. The precise mechanism by which Doxorubicin induces senescence in cells is not yet fully understood. However Doxorubicin is toxic to cells, which diminishes its therapeutic efficacy (57).

1.4 Research question and hypothesis

The role of senescent cells in OA is still not fully understood. Consequently targeted therapies which could truly halt or reverse the progress of scenescence are not available. Hence it would be important to better understand how senescence is induced and if and how it can be influenced by availabel or new treatments. Protocols to induce senescence in human cells or

cells from mice/rats are already available. However, research on human cells is limited to to ethical reasons and mice or rats do not commonly suffer from naturally occuring OA which indicates that studies on OA pathophysiology should be performed using an animal model more closely resembling human OA. The aim of this diploma thesis was therefore to develop an ovine in vitro model of chondrocyte and synoviocyte senescence using cells obtained post-mortem from 3 adult sheep.

Hypothesis: Protocols for inducing senescence in human and mouse/rat cells can be adapted to induce senescence in sheep.

2. Material and Methods

2.1. Materials, reagents, and equipment used in the study

Table 1: Materials

materials	**company**
50 ml Falcon tubes	sterile, Sarstedt
Cell strainer (100 µm)	Greiner BioOne
Cryovial floats	Sarstedt
Cryovials	Sarstedt
Eppendorf tubes (2 ml)	Sarstedt
Petri dishes	Sarstedt
Pipettes (1µl-100µl)	EPPENDORF; Deutschland
Pipettes (5ml, 10 ml, 25 ml)	sterile, Sarstedt
Scalpel	Swann-Morton, B.Braun
Sterile surgical instruments	Equine Clinic (University of Veterinary Medicine Vienna9
Stir bar	IKA (Modell: Colorsquid)
T-flasks (175 cm^2, 100 cm^2)	Sarstedt
Well plates	Sarstedt

Table 2: Reagents

reagents	**company**
0,5 % Trypsin- 0,02% EDTA	Biochrom
1% Amphotericin B	Biochrom, Cambridge, UK
1% PS (Penicillin-Streptomycin)	Sigma-Aldrich, St. Louis, MO, USA
10 % FCS (Fetal calf serum)	Capricorn
Beta-mercaptoethanol	Sigma Aldrich
Chloroform	SIGMA-ALDRICH
Collagenase solution (1 mg/mg)	Gibco (Thermo Fisher Scientific (Life Technologies))
DEPC water	Invitrogen (Thermo Fisher Scientific (Life Technologies))
Dexamethasone	Sigma Aldrich
DMEM (Dulbecco's Modified Eagle Medium)	Gibco
DNase buffer	Thermo Fisher Scientific (Life Technologies)
DNase enzyme	Thermo Fisher Scientific (Life Technologies)
DNase inactivation solution	Thermo Fisher Scientific (Life Technologies)
Doxorubicin	Sigma Aldrich
Glycogen	Thermo Fisher Scientific (Life Technologies)
Isopropanol	Carl Roth
MTT - 3 – (4,5 – Dimethythiazol – 2- yl) – 2,5 – diphenyltetrazoliumbromid	CellTiter96® Aqueous, Promega Cooperation
Nuclease-free water	Invitrogen (Thermo Fisher Scientific (Life Technologies)
PBS (Phosphate-buffered saline)	Gibco (Thermo Fisher Scientific (Life Technologies))
PBS +/+ (PBS with serum supplement)	Gibco (Thermo Fisher Scientific (Life Technologies))

RNA treatment mixture	Invitrogen (Thermo Fisher Scientific (Life Technologies))
StemMacs Basismedia	Mittenyi Biotec
Trizol	Invitrogen (Thermo Fisher Scientific (Life Technologies))

Table 3: Equipment

equipment	**company**
Centrifuge	Rotina 420R, Hettich, Westfalenm Deutschland
Countess counting chamber	The Countess® II FL Automated Cell Counter
Evos FL Auto	Life Technologies
Graph Pad Prism v.6.01	GraphPad Software, San Diego, CA, USA
Incubator	ThermoFisher
Laminar Flow Workbench	Herasafe KS12
Microscope	Olympus CKX31
Pipetboy	EPPENDORF; Deutschland
Primer3 software	Whitehead Institute for Biomedical Research
qPCR One-Step Eva Green kit	Bio& Sell, Feucht, Germany
Quant Studio software	Invitrogen, Thermo Fischer Scientific
Nanophotometer	Implen GMBH
Vortex mixer	MS3 basic (IKA); Deutschland

2.2. Sample collection

The samples for this experiment were obtained from 3 female Merino sheep, aged 2-5 years. The ethics approval was granted by the in-house ethics committee and the Federal Ministry of Education, Science, and Research (Animal Experimentation Number BMWF-68.205/0100-V/3b/2018). The cartilage from the sheep was collected post mortem after euthanasia using T61 following sedation with 0.3 ml of Domosedan and 0.3 ml of Butorphanol, and anaesthesia induction with Thiopental. The knee joints were shaved and prepared aseptically. Subsequently, they were dissected with a sterile scalpel, and cartilage was harvested from the femoral condyles. The harvested cartilage flakes were placed in a 50 ml Falcon tube containing PBS +/+ and 1% PS and 1% Amphothericin.

2.2.1. Isolation of cartilage cells from cartilage tissue

50 ml of a ready-to-use collagenase solution was prepared in a final concentration of 1 mg/mL. Additionally, three Petri dishes were prepared. One was used to place the surgical instruments for cutting the cartilage. The PBS containing the cartilage flakes was transferred from the Falcon tube, which was used for transporting the cartilage to the laboratory, to the second Petri dish under sterile conditions in the laminar flow workbench. There, the cartilage was minced into 2x2mm-sized pieces using a scalpel and transferred to a sterile beaker for digestion in the collagenase solution. The third dish was used for tissue waste. Digestion was carried out with continuous stirring using a magnetic stirrer for 4-6 hours in a cell culture incubator at 37°C until the cartilage was completely digested. Subsequently, the solution containing the digested cartilage was transferred through a cell strainer (to remove any remaining cartilage debris) into a 50 ml Falcon tube, washed twice with 40 ml PBS, and then the cartilage cells were resuspended in 25 ml of DMEM (containing 10% FCS, 1% PS, 1% Amphotericin) in a T175 cell culture flask and cultured at 37°C, 5% CO_2. For further processing until the 1st passage, macroscopic and microscopic examinations for contamination were conducted daily until Day 7. On Day 2, the cells were washed twice and 20 ml of new culture medium was added. To wash the cells, the medium was removed, and 20 ml of PBS were added using a pipette. The flask was gently swayed, and then the PBS was aspirated, and fresh medium was added. From this point onwards, the culture medium was changed twice a week. The medium was removed using a pipette, and 20 ml of new medium were added to the 175 cm^2 cell culture flask. The 1st passage was performed when the colony confluence reached 80%.

2.3. Introduction of Senescence in Chondrocytes and Synoviocytes in vitro

2.3.1. Cells in high passages

In order to induce cellular senescence without chemical reagents, the cells were subjected to high passaging to promote senescence. The high passage cells, as described in the prolieferation assay, freezing and thawing, and cell counting sections, were further used to compare the proliferation rate of high passage cells undergoing senescence with the proliferation rate of cells from the same donor in low passage, which had not yet entered senescence. For passaging, the medium was aspirated using a pipette. PBS was added according to the volume of the medium, and the flask was gently swayed. The PBS was aspirated, and a second washing step was performed. After aspirating the PBS, an appropriate amount of Trypsin-EDTA was added to the cell culture flask, according to the flask size. The Trypsin was evenly distributed in the culture vessel. The culture vessel was then incubated in a CO_2 incubator for 6 minutes. After the 6-minute incubation, the culture vessel was removed from the incubator and swayed. The bottom of the vessel was tapped gently with the fingers to facilitate cell detachment, and the cell detachment was examined macroscopically and microscopically. To inactivate the Trypsin, culture medium was added in the same volume as Trypsin. The cell suspension was transferred from the culture vessel into appropriately labelled 15 ml Falcon tubes. The culture vessel was rinsed with PBS, using an amount equivalent to the medium volume. The PBS containing potentially remaining cells was collected using a pipette and added to the Falcon tubes. The Falcon tubes were then centrifuged at 427g (2000 rpm) for 5 minutes. After centrifugation, the Falcon tubes were removed from the centrifuge, and the supernatant was aspirated. New culture vessels were labelled and filled with culture medium according to their size. To the Falcon tube, 2 ml of culture medium were added to resuspend the cell pellet. From the 2 ml in the Falcon tube, 1 ml was added to the corresponding culture vessel containing culture medium. The other 1 ml was discarded as the goal was to avoid over-seeding with too many cells, as they require sufficient space to grow and expand. The presence of cells was checked under the microscope, and the prepared culture vessels with cells were placed in the incubator. This process was repeated two to three times per week. The colony confluence was always checked to ensure it reached 80% before passaging.

The samples of the three donors were all passaged in the same manner.

2.3.2. Cryopreservation and thawing

The cells were frozen for two main purposes. Firstly, they served as a backup in case any issues arose during the high passaging process, ensuring that the cells could be thawed and utilized if needed. For this reason, cells from all three donors sheep 1, sheep 2, and sheep 3 were frozen at passages 20, 25, 30, and 35 to create backups at different high passages for each donor. This ensured that a reserve of cells was available in case of any issues or experimental requirements in the future. By preserving cells at various passages, it could be maintained a repository of cells from different stages of growth and senescence, enabling continued studies and comparisons between passages. Secondly, by freezing the cells and subsequently thawing them, it was determined whether they retained their proliferative capacity in higher passages, thus assessing their usefulness for future experiments. This process allowed for the evaluation of cell viability, recovery, and growth potential following cryopreservation, providing valuable information on the cells' suitability for ongoing studies. Cells from donor sheep 1, which were already frozen at passages 31 and 43, were utilized to test their viability after thawing due to their high passages.

For freezing the cells were resuspended in freezing medium (90%FCS, 10% DMSO). The cryovials were labelled, and 1 ml of cell suspension was transferred into each cryovial. The cryovials were placed in a Mr. Frosty and frozen at 80°C.

The cells from sheep 1 at Passages 31 and 43 were thawed and observed under the microscope for 7 days. For the thawing test the cryovials to be thawed were placed in the water bath. When the cell suspension was completely thawed, the cryovials were transferred to the bench, and the cell suspension was pipetted to a 15 ml Falcon tube. 2 ml of culture medium was added per 1 ml of cell suspension. The Falcon tubes were centrifuged at 427g for 5 minutes. The supernatant was aspirated, and the cells were resuspended in PBS. The Falcon tubes were centrifuged again in the same settings as before. The cells were resuspended in culture medium and seeded in the culture flask. The cells were then placed in the incubator.

2.3.3. Dexamethasone and Doxorubicin

To test the induction of senescence through chemical means, three different titration assays were performed with cells of sheep 1, sheep 2 and sheep 3 in low passage using Dexamethasone and Doxorubicin.

In the long-term titration assay, different concentrations of Dexamethasone and Doxorubicin were added to the well plates. The aim was to determine the optimal concentration of these chemicals for inducing senescence without causing cell damage. These well plates were also utilized to compare the effectiveness of Dexamethasone and Doxorubicin in inducing senescence. The assessment of senescence in the cells was carried out using qPCR and MTT assays (see qPCR and MTT chapters).
The short-term titration assay, which was conducted exclusively with Dexamethasone, aimed to determine the duration of Dexamethasone treatment required to induce senescence in chondrocytes. Low passage chondrocytes of sheep 1 and sheep 3 were used. Time points of 24 hours, 48 hours, and 72 hours were selected, and the chondrocytes were subsequently assessed for senescence using qPCR and MTT assays.
The 3-day and 6-day titration assay with Dexamethasone was conducted to ascertain the optimal duration of dexamethasone treatment for inducing senescence in chondrocytes and synoviocytes. However, in this instance, the RNA was harvested only after 3 days and 6 days, followed by performing qPCR.

First 12 (6 for chondrocytes and 6 for synoviocytes) well plates for the long-term titration assay and 6 well plates for the short-term titration assay were prepared. The cells were counted (see chapter cell counting), and the amount of cell suspension per well was calculated to have 1000 cells per well. Low passage chondrocytes and synoviocytes from all three donors were used in the long-term assay. In the short-term assay chondrocytes from sheep 1 and sheep 3 were used. For both assays, the wells were first filled with the cell suspension using a pipette. Subsequently, Dexamethasone and Doxorubicin were added to the wells based on the specific assay requirements.

2.3.3.1. Dexamethasone

2.3.3.1.1. Long-term titration assay with Dexamethasone

The calculated cell suspension of 1000 cells per well in StemMacs medium from donors sheep 1, sheep 2, and sheep 3 was pipetted separately into each well of the well plates according to the scheme depicted in the Table 5. A total of 6 well plates were used, three for chondrocytes with Dexamethasone, three for synoviocytes with Dexamethasone, for each donor one well plate per donor. Subsequently, Dexamethasone was added in different concentrations and mixed well with the cell suspension. The concentrations of 20 µM, 10 µM, 5 µM and 1 µM

Dexamethasone were added, as indicated in the table 5. Each column represented a different concentration of Dexamethasone for each donor. This day was designated as "Day 1" in the Table 6. Between the designated days, the well plates were stored in the incubator at 37°C.

sheep 1/2/3 low passage 20 µM Dexamethasone	sheep 1/2/3 low passage 10 µM Dexamethasone	sheep 1/2/3 low passage 5 µM Dexamethasone	sheep 1/2/3 low passage 1 µM Dexamethasone	MTT
sheep 1/2/3 low passage 20 µM Dexamethasone	sheep 1/2/3 low passage 10 µM Dexamethasone	sheep 1/2/3 low passage 5 µM Dexamethasone	sheep 1/2/3 low passage 1 µM Dexamethasone	
sheep 1/2/3 low passage 20 µM Dexamethasone	sheep 1/2/3 low passage 10 µM Dexamethasone	sheep 1/2/3 low passage 5 µM Dexamethasone	sheep 1/2/3 low passage 1 µM Dexamethasone	
sheep 1/2/3 low passage 20 µM Dexamethasone	sheep 1/2/3 low passage 10 µM Dexamethasone	sheep 1/2/3 low passage 5 µM Dexamethasone	sheep 1/2/3 low passage 1 µM Dexamethasone	qPCR
sheep 1/2/3 low passage 20 µM Dexamethasone	sheep 1/2/3 low passage 10 µM Dexamethasone	sheep 1/2/3 low passage 5 µM Dexamethasone	sheep 1/2/3 low passage 1 µM Dexamethasone	
sheep 1/2/3 low passage 20 µM Dexamethasone	sheep 1/2/3 low passage 10 µM Dexamethasone	sheep 1/2/3 low passage 5 µM Dexamethasone	sheep 1/2/3 low passage 1 µM Dexamethasone	

Table 4 Dexamethasone assay

On the 3rd and 5th day after the cells were seeded, the media containing Dexamethasone were replaced with new media. The well plate was inverted with a swift motion, and the liquid contents were collected using absorbent towels placed on the working bench. The well plates were handled carefully and the liquid contents were discarded without the towels coming into direct contact with the well plates. The cell pellets were left in the wells, and the same concentrations Dexamethasone were added again to the wells, following the same protocol as on Day 1. After the media change, the well plates were returned to the incubator with the same settings.

On Day 7, Dexamethasone was removed by again inverting the well plates to discard the liquid content. Subsequently, healthy DMEM medium was added to all the wells, and the well plates

were placed back in the incubator. On Day 10, a medium change was performed using the same procedure, and DMEM medium was added to the wells once again. On Day 10, eight wells that were previously left empty were filled with healthy cells in DMEM medium from all three donors. These wells served as the control group.
On Day 13, an MTT assay was conducted, and RNA was harvested for qPCR analysis (see MTT and qPCR chapters). The blue-marked wells in the table 5 were used for the MTT assays, while the white-marked wells were utilized for the qPCR analysis. With the synoviocytes only the qPCR was performed. Please refer to Table 6 for an overview of the steps.

Day 0	Day 1	Day 3	Day 5	Day 7	Day 10	Day 13
seed 1000 cells per well sheep 1/2/3 low passage	add Doxurrubicin and dexamethasone in different concentrations	change the media	change the media	change to healthy medium all the conditions	change medium all conditions; seed healthy	MTT/harvest RNA

Table 5 Plan long-term titration assay with Dexamethasone

2.3.3.1.2. Short-term titration assay with Dexamethasone

Also in this case, 1000 cells were seeded in StemMacs per well. A total of 6 well plates were used: two for performing an MTT assay and qPCR after 24 hours one with chondrocytes of sheep 1 and one with chondrocytes of sheep 3, two for performing an MTT assay and qPCR after 48 hours one with chondrocytes of sheep 1 and chondrocytes with cells of sheep 3, and two for performing an MTT assay and qPCR after 72 hours one with chondrocytes of sheep 1 and one with chondrocytes of sheep 3. The blue-marked wells in the Table 7 were used for the MTT assays, while the white-marked wells were utilized for the qPCR analysis. Each of the six plates was filled with four columns of chondrocytes from donor sheep 1 and four columns of chondrocytes from donor sheep 2. The starting day, referred to as "Day 1," was when Dexamethasone was added to the cell suspension in four different concentrations (20 µM, 10 µM, 5 µM, and 1 µM) for each donor and each plate, and mixed accordingly. Empty wells were filled with healthy chondrocytes in DMEM medium from both donors, for each 3 wells were used. These wells served as the control group. Based on the well plate the cells were placed in, an MTT assay or RNA harvest for qPCR was conducted after 24 hours, 48 hours and 72 hours. Please refer to Table 8 for an overview of the steps.

sheep 1/3 low passage 20 µM Dexamethasone	sheep 1/3 low passage 10 µM Dexamethasone	sheep 1/3 low passage 5 µM Dexamethasone	sheep 1/3 low passage 1 µM Dexamethasone	MTT
sheep 1/3 low passage 20 µM Dexamethasone	sheep 1/3 low passage 10 µM Dexamethasone	sheep 1/3 low passage 5 µM Dexamethasone	sheep 1/3 low passage 1 µM Dexamethasone	
sheep 1/3 low passage 20 µM Dexamethasone	sheep 1/3 low passage 10 µM Dexamethasone	sheep 1/3 low passage 5 µM Dexamethasone	sheep 1/3 low passage 1 µM Dexamethasone	
sheep 1/3 low passage 20 µM Dexamethasone	sheep 1/3 low passage 10 µM Dexamethasone	sheep 1/3 low passage 5 µM Dexamethasone	sheep 1/3 low passage 1 µM Dexamethasone	qPCR
sheep 1/3 low passage 20 µM Dexamethasone	sheep 1/3 low passage 10 µM Dexamethasone	sheep 1/3 low passage 5 µM Dexamethasone	sheep 1/3 low passage 1 µM Dexamethasone	
sheep 1/3 low passage 20 µM Dexamethasone	sheep 1/3 low passage 10 µM Dexamethasone	sheep 1/3 low passage 5 µM Dexamethasone	sheep 1/3 low passage 1 µM Dexamethasone	

Table 6 Short-term assay Dexamethasone 24/48/72 hours

Day 0	Day 1	Day 2	Day 3	Day 4
seed 1000 cells per well sheep 1/3 low passage	add Dexamethasone in different concentrations seed healthy (ctr.)	MTT 24h Harvest RNA 24h	MTT 48h Harvest RNA 48h	MTT 72h Harvest RNA 72h

Table 7 Short-term titration assay with Dexamethasone

2.3.3.1.3. 3-day and 6-day titration assay with Dexamethasone

The 3-day and 6-day titration assay with Dexamethasone was conducted using chondrocytes and synoviocytes from sheep 1, sheep 2, and sheep 3. Concentrations of 20 µM, 10 µM, 5 µM, and 1 µM Dexamethasone were utilized (refer to Table 9). For each well in 12-well plates, 1000 cells were seeded in StemMacs, as indicated in Table 10 as Day -3. Six wells were used for chondrocytes, once for each of the three donors, to harvest RNA after 3 days and once after 6 days. Similarly, for synoviocytes, another six wells were prepared, once for each donor,

where RNA was harvested after 3 days and once after 6 days. As per Table 10, on Day 0, Dexamethasone was added in varying concentrations, and healthy chondrocytes and synoviocytes were seeded for each donor, serving as the control group. Following the RNA harvest on Day 3 and Day 6, a qPCR analysis was performed.

sheep 1/2/3 low passage 20 µM Dexamethasone	sheep 1/2/3 low passage 10 µM Dexamethasone	sheep 1/2/3 low passage 5 µM Dexamethasone	sheep 1/2/3 low passage 1 µM Dexamethasone	qPCR
sheep 1/2/3 low passage 20 µM Dexamethasone	sheep 1/2/3 low passage 10 µM Dexamethasone	sheep 1/2/3 low passage 5 µM Dexamethasone	sheep 1/2/3 low passage 1 µM Dexamethasone	
sheep 1/2/3 low passage 20 µM Dexamethasone	sheep 1/2/3 low passage 10 µM Dexamethasone	sheep 1/2/3 low passage 5 µM Dexamethasone	sheep 1/2/3 low passage 1 µM Dexamethasone	

Table 8 Titration assay Dexamethasone 3 days and 6 days

Day -3	Day 0	Day 3	Day 6
seed 1000 cells per well sheep 1/3 low passage	add Dexamethasone in different concentrations seed healthy cells (ctr.)	Harvest RNA 72h	Harvest RNA 6 days

Table 9 Titration assay with Dexamethasone 3 days and 6 days

2.3.3.2. Doxorubicin

2.3.3.2.1. Long-term titration assay with Doxorubicin

The long-term titration assay with Doxorubicin was performed similarly to the long-term titration assay with Dexamethasone as described in 2.3.3.1.1. Condrocytes and synoviocytes were used. The concentrations 200 nM, 100 nM, 50 nM and 25 nM were used for Doxorubicin as described in Table 10.

sheep 1/2/3 low passage 200 nM Doxurrubicin	sheep 1/2/3 low passage 100 nM Doxurrubicin	sheep 1/2/3 low passage 50 nM Doxurrubicin	sheep 1/2/3 low passage 25 nM Doxurrubicin	MTT

sheep 1/2/3 low passage 200 nM Doxurrubicin	sheep 1/2/3 low passage 100 nM Doxurrubicin	sheep 1/2/3 low passage 50 nM Doxurrubicin	sheep 1/2/3 low passage 25 nM Doxurrubicin	
sheep 1/2/3 low passage 200 nM Doxurrubicin	sheep 1/2/3 low passage 100 nM Doxurrubicin	sheep 1/2/3 low passage 50 nM Doxurrubicin	sheep 1/2/3 low passage 25 nM Doxurrubicin	
sheep 1/2/3 low passage 200 nM Doxurrubicin	sheep 1/2/3 low passage 100 nM Doxurrubicin	sheep 1/2/3 low passage 50 nM Doxurrubicin	sheep 1/2/3 low passage 25 nM Doxurrubicin	qPCR
sheep 1/2/3 low passage 200 nM Doxurrubicin	sheep 1/2/3 low passage 100 nM Doxurrubicin	sheep 1/2/3 low passage 50 nM Doxurrubicin	sheep 1/2/3 low passage 25 nM Doxurrubicin	
sheep 1/2/3 low passage 200 nM Doxurrubicin	sheep 1/2/3 low passage 100 nM Doxurrubicin	sheep 1/2/3 low passage 50 nM Doxurrubicin	sheep 1/2/3 low passage 25 nM Doxurrubicin	

Table 10 Doxurubicin assay

2.3.3.3. Comparison Dexamethasone and Doxurubicin

After optimizing the timing and concentration for the use of Dexamethasone and Doxorubicin on chondrocytes and synoviocytes as described in chapters 2.3.3.1.and 2.3.3.2., a direct comparison between Dexamethasone and Doxorubicin was pursued. Both cell types were treated with Dexamethasone and Doxorubicin for 3 days. For chondrocytes treated with Dexamethasone, a concentration of 1 µM was used, and for synoviocytes, a concentration of 5 µM was applied. Doxorubicin was used at a concentration of 50 nM for both chondrocytes and synoviocytes. Subsequently, a qPCR was performed to assess the genexpression levels of p53, p21, SIRT1, and MMP1.

2.4. Proliferation assays

2.4.1. Cell counting and proliferation assay

The cell counting and proliferation assay were performed to compare the growth patterns of senescent cells and non-senescent cells. The cells were counted after being resuspended in 2 ml of medium following centrifugation (refer to the High Passaging chapter). A drop of the cell suspension was placed in an Eppendorf tube. From the Eppendorf tube, 10 microliters were transferred to a new Eppendorf tube and 10 microliters of Trypan blue were added. Then, 10 microliters from this mixture were loaded into one side of the Countess counting chamber. The cell count and viability (as indicated by the device per ml) were documented, and the process was repeated with the second side of the counting chamber. The average of the two

counts was calculated and multiplied by the millilitres in which the cells were resuspended, in order to calculate the total cell amount.

To determine cell proliferation 1x10^6 cells were seeded into a 175 cm² T-flask. The cells used were sheep 4 in Passage 35 and sheep 4 in Passage 5. And as a control sheep 2 Passage 5 and sheep 3 Passage 4. On Day 1 and Day 2, the cells were observed under the microscope. After three days, the cells were counted again as described above. The proliferative arrest of cells is considered an indicator of senescence. More detailed analysis of the influence of senescence on cell proliferation by qPCR or MTT assay, was not conducted due to time constrains of this thesis.

2.4.2. Microscopic phenotype

Photos of the cell cultures were taken to compare the visual characteristics of senescent cells and non-senescent cells. This visual analysis provided additional insights into the morphological differences between the cell populations, allowing for a comprehensive comparison of their phenotypic features. Photos were taken using the Evos FL Auto.

2.5. Senescence and cell viability assays

2.5.1. RNA Isolation

RNA isolation was performed to enable subsequent qPCR analysis. For the RNA isolation, which was conducted with cells from the wells marked in purple in the figure, 100 µl of Trizol and 1 µl of beta-mercaptoethanol were added per well to lyse the cells. Subsequently, the cell lysates from three wells with the same treatment were combined (300 µl) in a 2 ml Eppendorf tube and supplemented with 700 µl of Trizol plus 7 µl of beta-mercaptoethanol to make a total volume of 1 mL. The mixture was vortexed for five minutes at full speed and then centrifuged at 13,000 rpm for 10 minutes at 4°C. The resulting supernatant was carefully transferred to a new 2 ml Eppendorf tube, and 200 µl of chloroform (0.2 ml per 1 ml of Trizol) were added. After thorough shaking and a 5-minute incubation at room temperature, the sample underwent centrifugation for 15 minutes at 13,000 rpm and 4°C.

This centrifugation step led to the separation of the mixture into three distinct layers: a lower red phenol-chloroform layer, an interphase, and an upper aqueous phase. The aqueous phase, which contained the RNA, was collected by angling the tube at a 45° angle and carefully pipetting the solution out. Subsequently, the aqueous phase was diluted with an equal volume

of DEPC water. To further process the RNA, 0.8 volumes of isopropanol and 1 µl of glycogen were added to the aqueous phase DEPC water mixture. The resulting solution was mixed thoroughly by shaking and incubated for 10-15 minutes at 4°C. Following this incubation, the sample underwent another round of centrifugation at 13,000 rpm for 10 minutes at 4°C. The supernatant was discarded, and the RNA pellet was washed twice with 75% ethanol.

After washing, the sample was centrifuged for 5 minutes at 13,000 rpm at 4°C, and the supernatant was carefully removed. The RNA pellet was then air-dried for 5 minutes before being reconstituted with 20 µl of nuclease-free water. For the subsequent RNA treatment, a mixture was prepared for each sample. The mixture included 6 µl of nuclease-free water, 3 µl of DNase buffer, and 1 µl of DNase enzyme. Additional mixtures were prepared as needed for multiple samples. Each sample was treated with 10 µl of the RNA treatment mixture and incubated at 37°C for 20 minutes. After the incubation, 5 µl of DNase inactivation solution was added and the samples were incubated for an additional 2 minutes at room temperature.
Following the incubation, the samples were centrifuged at 13,000 rpm, 4°C for 3 minutes. From the resulting supernatant, 25 µl was carefully transferred to a 1.5 ml Eppendorf tube, which was then kept on ice until further RNA measurement.

2.5.2. qPCR

A qPCR (quantitative polymerase chain reaction) was performed to analyse gene expression levels of the genes of p53, p21, Catalase, LMNB 1, SIRT 1, TERT and some of the SAPS (IL-9, IL-8, IL-1beta and TNF alpha). The genes of matrix metalloproteinases MMP1 and MMP13, which can be released by SAPS, were also analysed. These genes were selected because the upregulation or downregulation of these genes can contribute to the induction and maintenance of the senescent state in cells. By studying the gene expression changes during senescence, it is possible to gain insights into the molecular mechanisms and signalling pathways involved in the senescence process. 100 ng/µl RNA per well was used for the qPCR reaction, which was performed with the qPCR One-Step Eva Green kit. The results were analysed using the QuantStudio software. The mRNA levels were calculated by first normalizing using the BestKeeper Index (Housekeeping genes used GAPD and RPBI) and then using the $2^{\wedge ct\Delta}$ method. All primers were designed using the Primer3 software.

2.5.3. MTT (3-(4,5-dimethylthiazol-2-yl)-2,5-diphenyltetrazolium bromide) cell viability/cytotoxicity assay

To measure the metabolic activity 50 µl CellTiter96® AQueous MTT reagent was added to each well containing the cells. MTT is a yellow tetrazolium dye that is taken up by metabolically active cells. The cells were incubated with the MTT reagent for 2-4 hours, at 37°C and 5% CO2. During this time, the MTT was converted to formazan crystals by the mitochondrial dehydrogenase enzyme present in viable cells.

Then, the absorbance of the formazan solution was measured using a spectrophotometer at a specific wavelength of 490 nm. The absorbance is proportional to the number of viable cells/metabolically active cells. The absorbance values obtained from wells with the different treatment conditions were compared to determine the relative cell viability in order to detect senescence. Wells with non-senescent cells were used as control.

2.6. Statistical Analysis

One way ANOVA, Dunnett test with a confidence intervall of 95% (column analysis), was performed for all comparisons using using Graph Pad Prism v.6.01
Unfortunately, no statistically significant results ($p < 0.05$) were achieved due to the low number of biological donors included into the study (n=3) and the high inter-individual donor variation. However, trends have been identified, which were compared and presented in the results in the vein of “descriptive statistics”.

3. Results

3.1. Introduction of Senescence and viability of chondrocytes

3.1.1. High passaging

3.1.1.1. Proliferation

The aim of the seeding test is to compare the proliferation of the high passages with that of the low passages. On Day 3, after seeding 1x10^6 cells per 175 cm² T-flask for donors sheep 1 P35, sheep 1 P5 and sheep 2 P5 different cell counts were obtained for each. The high passage cells from donor sheep 1 P35 exhibited a decrease in cell count, with 762,500 cells counted, corresponding to a loss of 23.75%. These cells did not proliferate but experienced cell death. In contrast, the low passage cells showed a cell count higher than the initially seeded number. Donor sheep 1 P5 had a cell count of 1,085,000 on day 3, representing a growth of 8.5%. Sheep 2 showed a cell count of 1,627,500, corresponding to a growth of 62.75%. Donor sheep 1 P5 had a lower cell count than donor sheep 2 P5, despite being at the same passage. It was observed that the cell count of the high passage 35 was lower on day 3 compared to day 1.

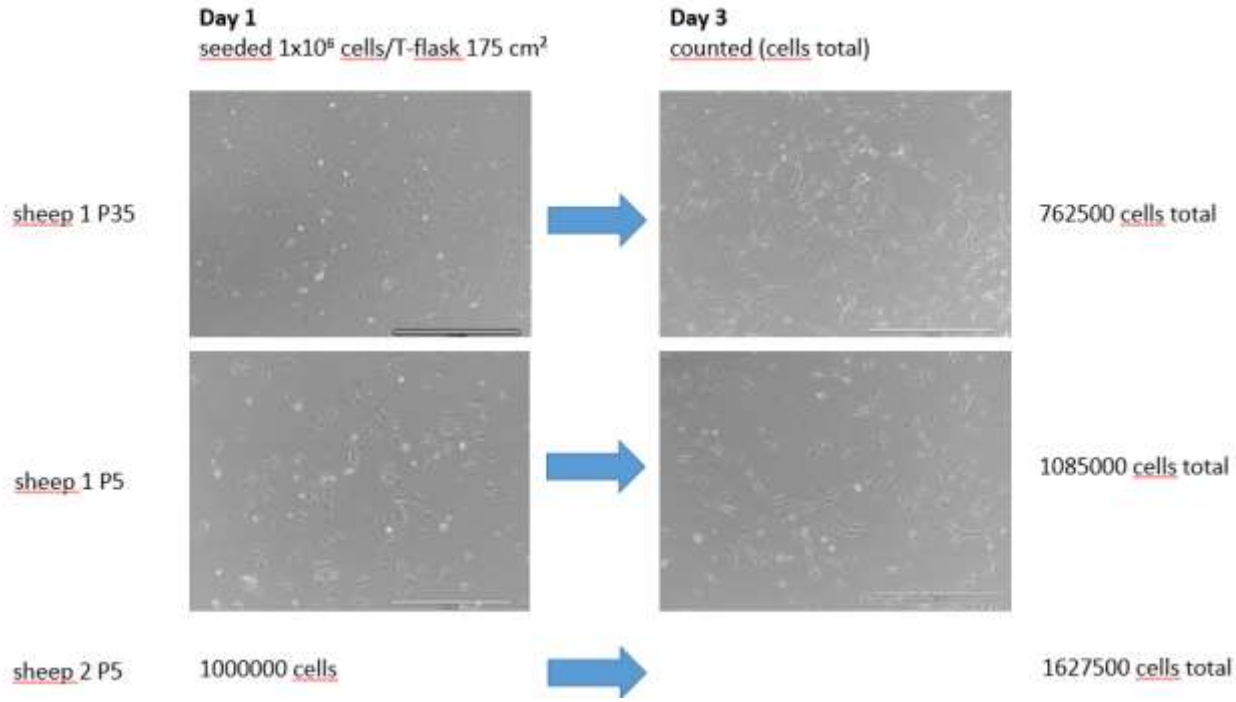

Figure 4 Results Prolieferation assay

3.1.1.2. Freezing and thawing

The objective of this experiment was to determine the proliferative capacity of cells at high passages after undergoing the process of freezing and thawing. The chondrocytes from donor sheep 1 at passage 49 did not exhibit cell growth after thawing. On Day 3 post-thaw, there were fewer cells compared to Day 1, and an increased presence of cell fragments was observed. Cell death occurred, and on day 6 post-thaw, only a few morphologically identifiable cells were visible. Some cell remnants could be detected under the microscope. There was no further cell proliferation taking place, and the cells could not be passaged.

In contrast, the chondrocytes from donor sheep 1 at passage 31 showed cell growth after thawing. On day 3 post-thaw, no differences were observed compared to day 1 post-thaw. By day 6, the cells had doubled in number and displayed typical chondrocyte morphology. The cell confluence in the T-flask reached 60%. In comparison, on day 1 post-thawing, there was a cell confluence of 10%. On day 7, the cells were successfully passaged for further experiments.

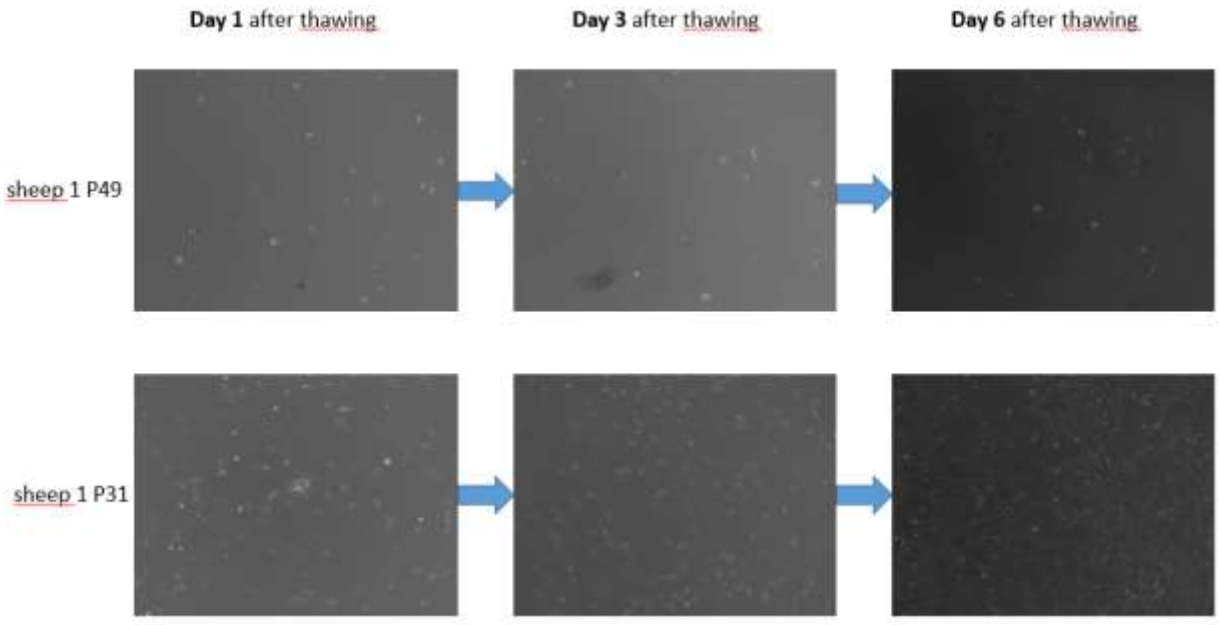

Figure 5 Microscopic observation freezing and thawing test

3.1.2. Dexamethasone

3.1.2.1. Long-term titration assay with Dexamethasone

3.1.2.1.1. qPCR

The qPCR was taken to have an insight on the genes which regulate senescence (TERT, Catalase, LMNB1, Sirt1, p53, p21, IL-6, IL-8, IL-1b, TNF alpha, MMP1 and MMP 13). Attention was given to identify which genes are either upregulated or downregulated and if they have an impact on each other.

In this test Doxorubicin and Dexamethasone were compared to find out which one is better to induce senescence with. Meaning which one is not causing harm to the cells or even cell death. Furthermore, this long-term assay should aim to determine the optimal concentration for inducing senescence. This information will be valuable for subsequent experiments that require cells in a senescent state, allowing for efficient and effective generation of senescent cells in vitro.

3.1.2.1.1.1. Chondrocytes-Dexamethasone

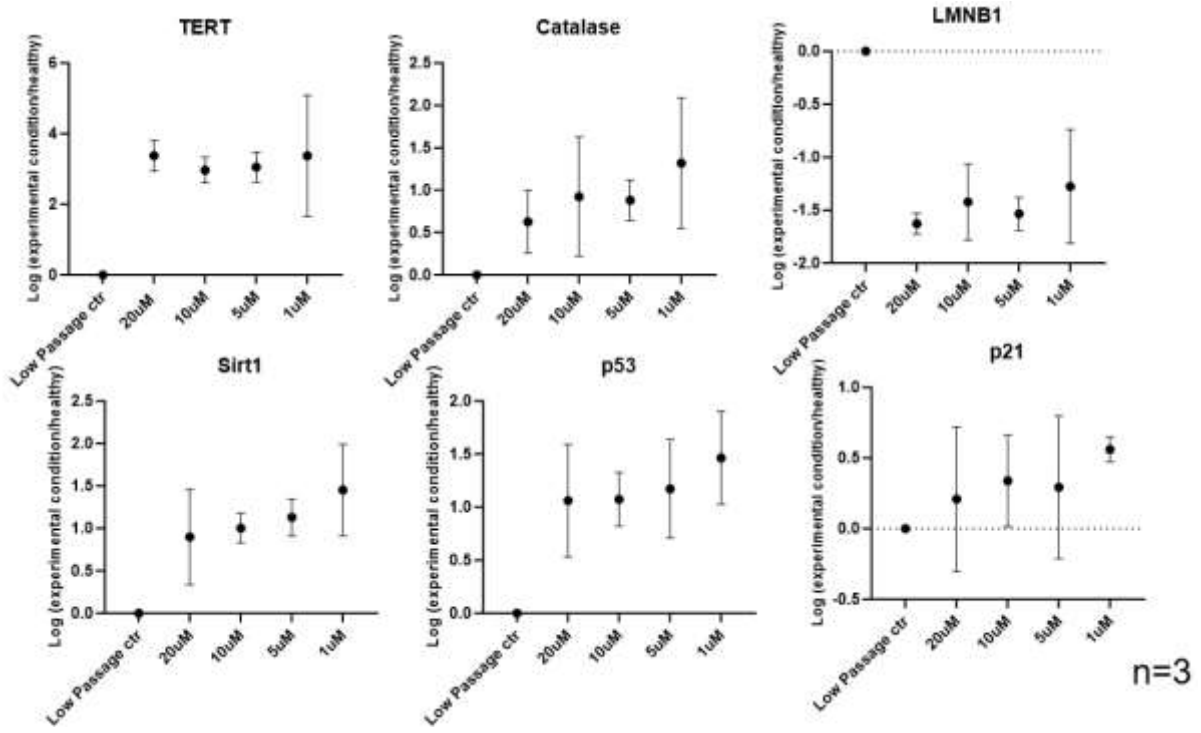

Figure 6 Scatterplots: qPCR long-term titration assay with Dexamethasone, Chondrocytes; no statistically significant results

These graphs depict the expression of various senescence-associated genes in chondrocytes relative to the concentrations (20 µM, 10 µM, 5 µM, and 1 µM) of Dexamethasone with which these chondrocytes were treated for 6 days. Among nearly all the genes, the highest

upregulation was observed at the concentration of 1 µM. However, a noticeable upregulation of gene expression can also be observed at the other concentrations. LMNB1 shows a downregulation of gene expression.

3.1.2.1.2. Cell viability assay (MTT) – Chondrocytes with Dexamethasone

To assess the metabolic activity and determine whether the chondrocytes survived the treatment and maybe transitioned into senescence or the cells entered cell death, an MTT test was performed. Metabolically active cells take up a yellow tetrazolium dye, with which they were incubated for 2-4 hours, and convert it into formazan crystals during the incubation period. The absorption of the formazan solution was measured using a spectrometer at 490 nm. The measured absoption levels (optical density) correlates with the number of metabolically active cells.

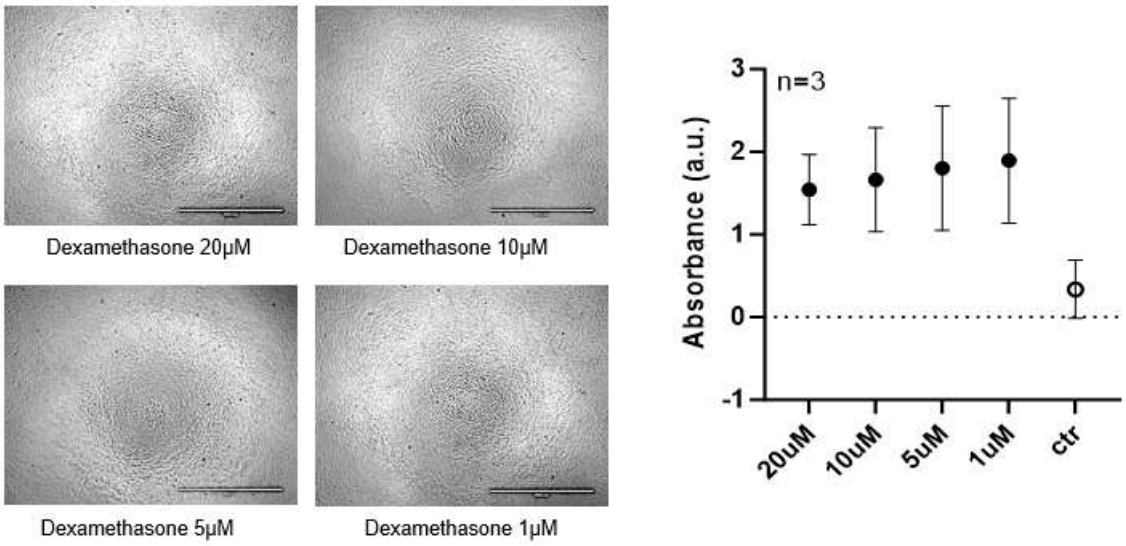

Figure 7 Scatterplots: MTT long-term titration assay with Dexamethasone, Chondrocytes; no statistically significant results

This experiment demonstrates the measurement of optical density at 490 nm of the formed formazan from MTT by chondrocytes in relation to the various concentrations (20 µM, 10 µM, 5 µM, and 1 µM) of Dexamethasone, in which the chondrocytes remained for 6 days and then dor more 6 days in healthy medium. The absorbance has remained relatively consistent across the different concentrations, staying between 1.5 and 2 for all four concentrations. None of the concentrations exhibit a toxic effect on chondrocytes, as no decrease in cell proliferation can be observed. Visually under the microscope no decrease of proliferation or dead cells can be

observed for any of the concentrations. It is evident that as the concentration increases, the absorption decreases but the decrease is lower than with Doxorubicin. Cell viability seems to increase with treatment of Dexamethasone, as it is noticeably apparent that the absorbance of the control group is lower than that of the treated cells.

3.1.2.2. Short term titration assay with Dexamethasone

3.1.2.2.1. qPCR

For the short-term assay, a qPCR was performed for the same reasons as in the long-term assay, aiming to gain insight into the either upregulation or downregulation of senescence associated genes (TERT, LMNB1, Sirt1, p53, p21). This was done to determine which cells transitioned into a senescent state through the treatment of Dexamethasone. The difference in the short-term assay, however, is that a qPCR was conducted after 24, 48, and 72 hours to determine the duration for which the cells should be treated with Dexamethasone. Various concentrations were also used here to identify the most effective combination of concentration and treatment duration of Dexamethasone to induce cells into senescence.

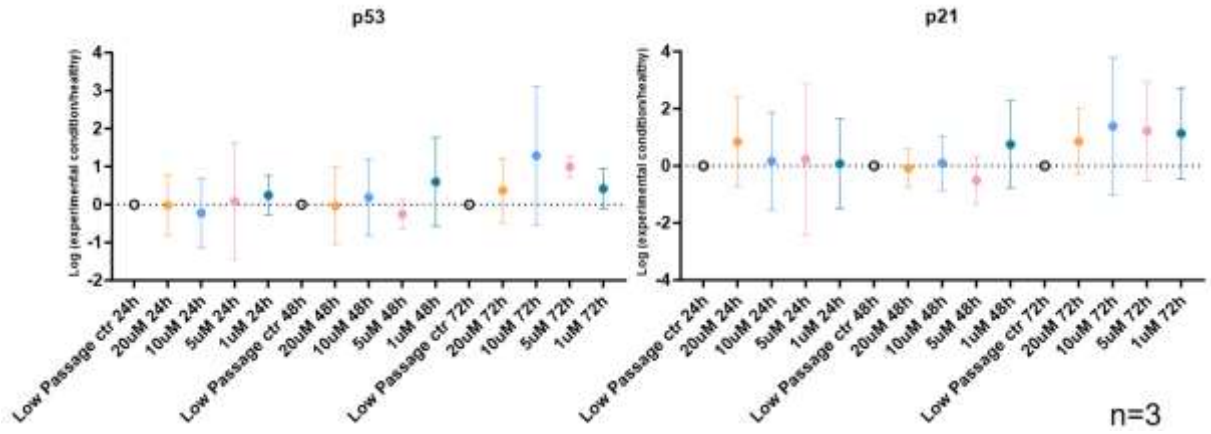

Figure 8 Scatterplots: qPCR short-term titration assay with Dexamethasone, Chondrocytes; no statistically significant results

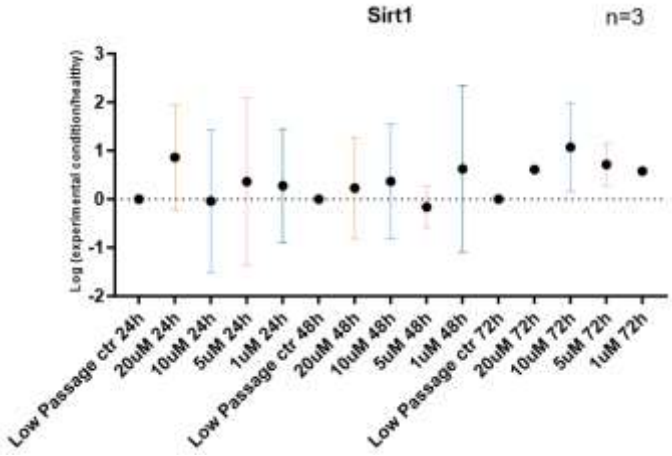

Figure 9 Scatterplots: qPCR short-term titration assay with Dexamethasone, Chondrocytes; no statistically significant results

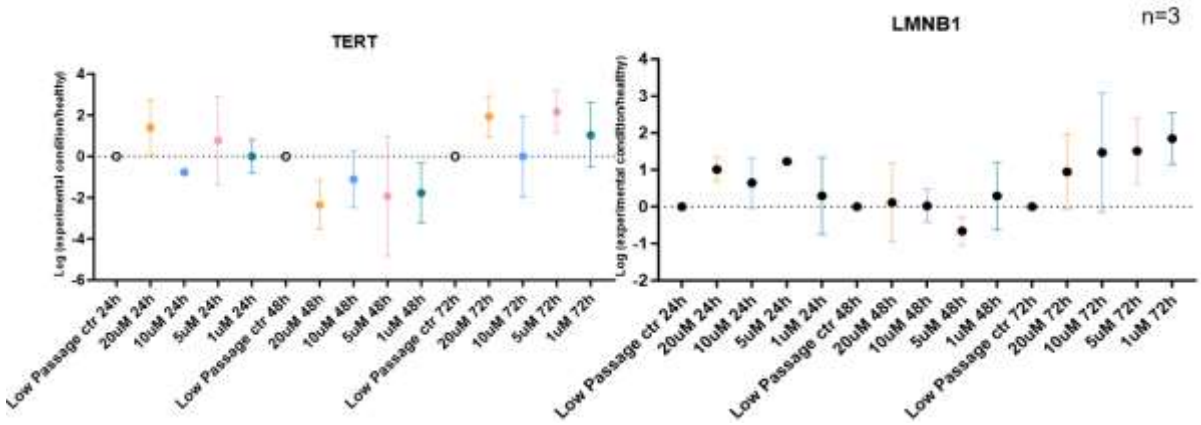

Figure 10 Scatterplots: qPCR short-term titration assay with Dexamethasone, Chondrocytes; no statistically significant results

These graphs depict the expression of senescence-associated genes in chondrocytes relative to the concentrations (20 µM, 10 µM, 5 µM, and 1 µM) of Dexamethasone and the treatment duration of 24 hours, 48 hours, and 72 hours. It is immediately noticeable that the gene expression for all concentrations is highest at a treatment duration of 72 hours. Chondrocytes appear to transition into senescence after at least 72 hours of Dexamethasone treatment.

3.1.2.2.2. Cell viability assay (MTT)

To evaluate the metabolic activity and determine the most suitable treatment duration of Dexamethasone among the three (24 hours, 48 hours, and 72 hours), an MTT test was conducted.

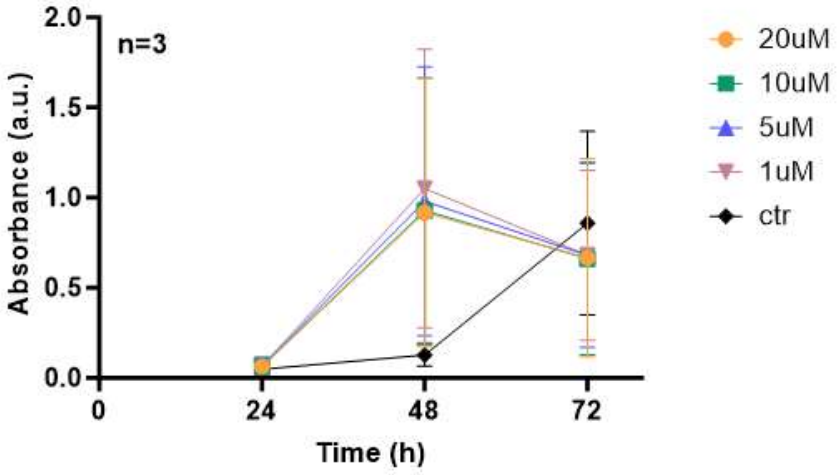

Figure 11 MTT short-term titration assay with Dexamethasone, Chondrocytes; no statistically significant results

This experiment illustrates the measurement of optical density at 490 nm of the formed formazan from MTT by chondrocytes treated with different concentrations (20 µM, 10 µM, 5 µM, and 1 µM) of Dexamethasone, depending on the duration (24 hours, 48 hours, and 72 hours) of treatment with Dexamethasone. Across all four concentrations, an increase in absorption is observed up to the 48-hour mark, with a stronger initial increase between 24 hours and 48 hours than after 48 hours. (Figure 11) After 48 hours, a decrease in absorption is noticeable for all four concentrations, leading to the 72-hour mark. At a concentration of 1 µM Dexamethasone, the highest measured absorption is observed at 48 and 72 hours, while a concentration of 20 µM Dexamethasone resulted in the lowest absorption measurement. The proliferation of the control group increases progressively over time.

3.1.2.3. 3-day and 6-day titration assay with Dexamethasone

3.1.2.3.1. qPCR

This qPCR was carried out to determinate which concentration of Dexamethasone (20, 10, 5 and 1 µM) at day 3 and 6 of incubation in chondrocytes and synoviocytes successfully induces senescence in vitro.

3.1.2.3.1.1. Chondrocytes

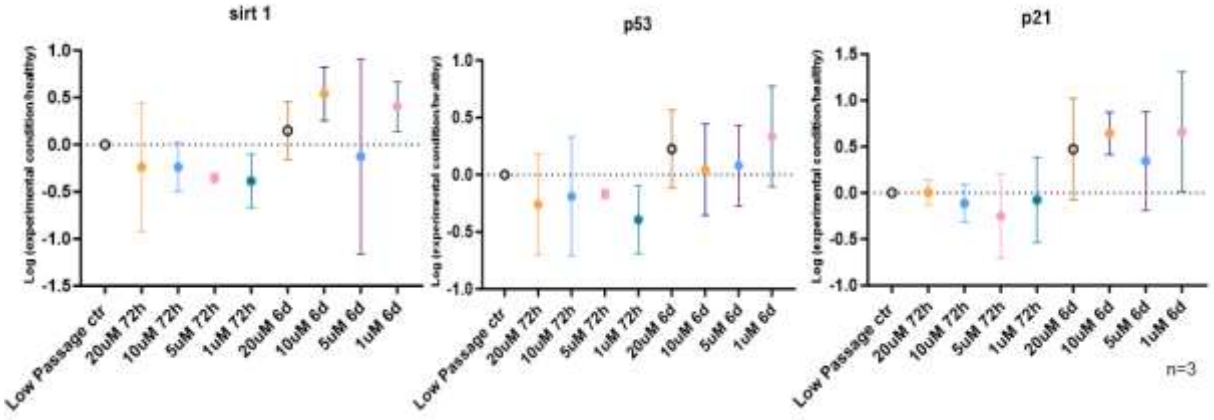

Figure 12 Scatterplots: qPCR 3-day and 6-day titration assay with Dexamethasone, Chondrocytes; no statistically significant results

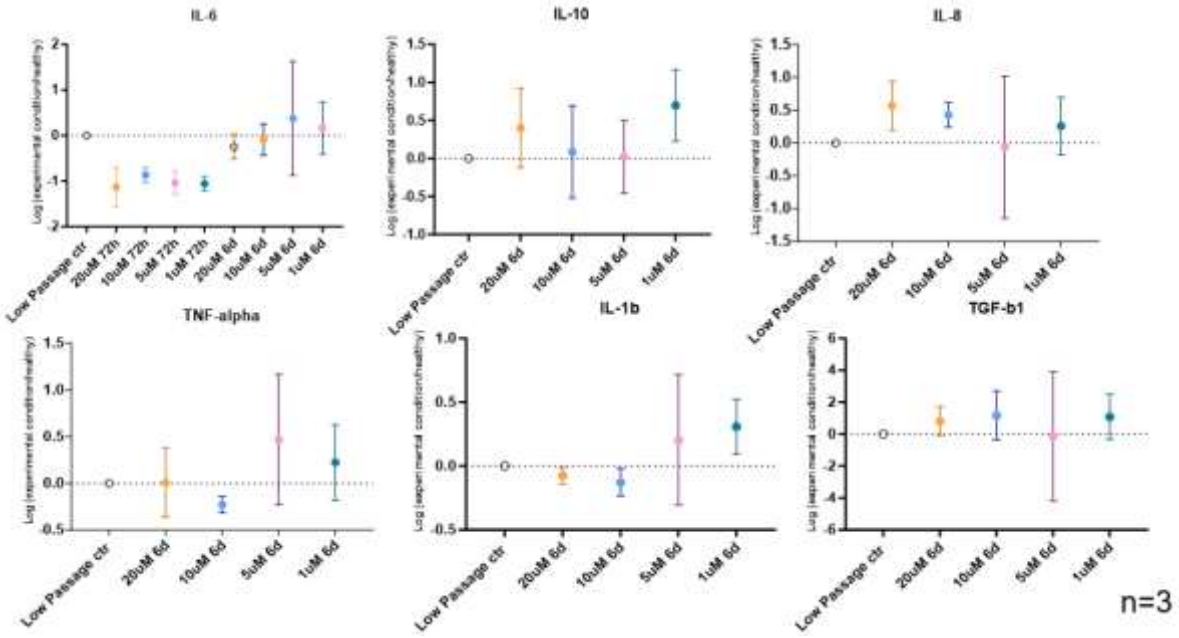

Figure 13 Scatterplots: qPCR 3-day and 6-day titration assay with Dexamethasone, Chondrocytes; no statistically significant results

These graphs illustrate the expression of senescence-associated genes in chondrocytes relative to the concentrations (20 µM, 10 µM, 5 µM, and 1 µM) of Dexamethasone and the duration in which they were treated either for 3 days and 6 days. The gene expressions of all genes were downregulated after 3 days, and chondrocytes did not exhibit senescence-associated gene expression. On day 6, most genes show an upregulation of senescence-associated genes. Particularly noteworthy is that a concentration of 1 µM Dexamethasone leads to an upregulation of gene expression for all genes. Especially for the three most senescence-associated genes, SIRT1, p53, and p21, chondrocytes show a distinct expression at a concentration of 1 µM. At concentrations of 20 µM, 10 µM, and 5 µM, at least one of the senescence-associated genes is consistently downregulated after 6 days.

3.1.2.3.1.2. Synoviocytes

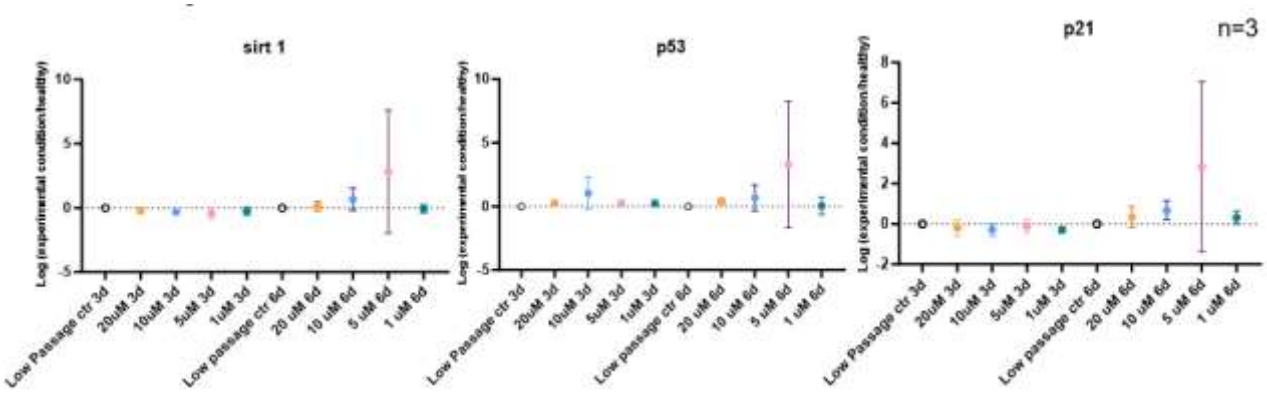

Figure 14 Scatterplots: qPCR 3-day and 6-day titration assay with Dexamethasone, Synoviocytes; no statistically significant results

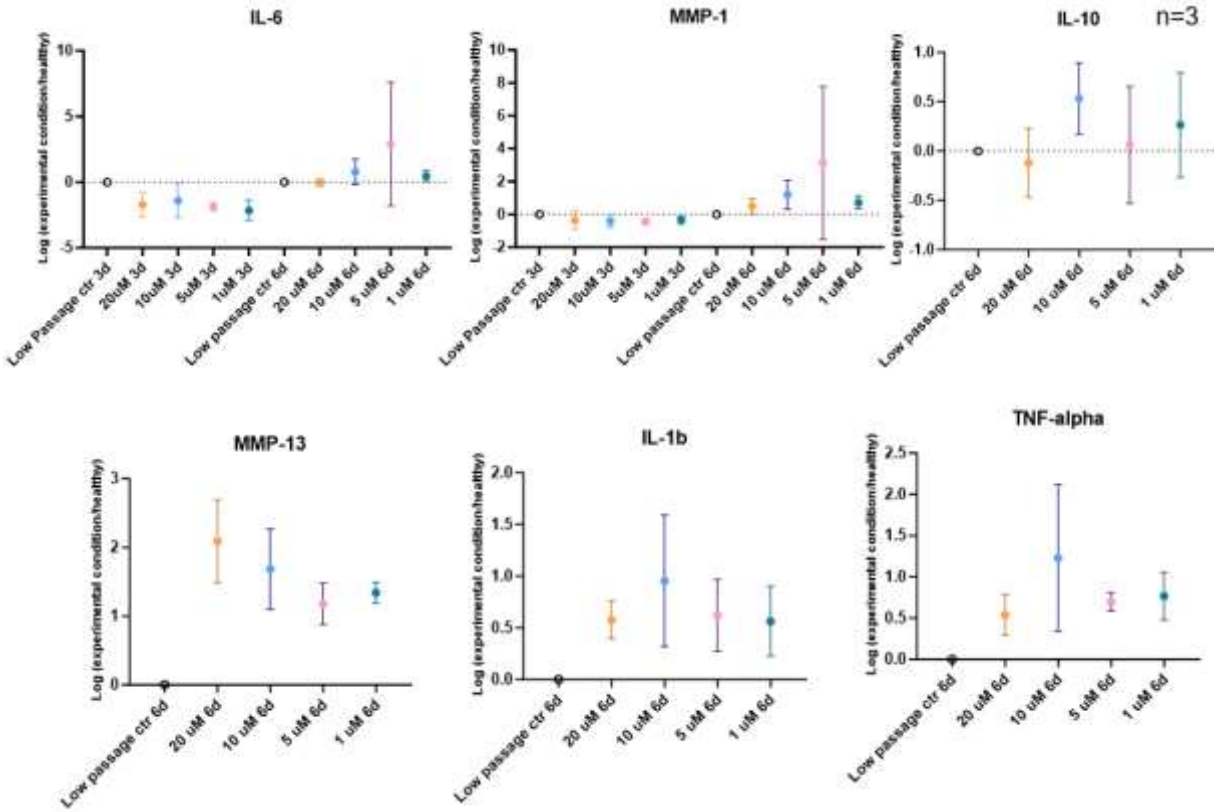

Figure 15 Scatterplots: qPCR 3-day and 6-day titration assay with Dexamethasone, Synoviocytes; no statistically significant results

These graphs illustrate the expression of senescence-associated genes in synoviocytes relative to the concentrations (20 µM, 10 µM, 5 µM, and 1 µM) of Dexamethasone and the duration in which they were treated either for 3 days and 6 days. The synoviocytes show a similar pattern of gene expressions with concentrations and duration as the chondrocytes. However, it is noticeable that the strongest upregulation is not at a concentration of 1 µM as seen in chondrocytes, but at a concentration of 5 µM. This is most evident in the genes SIRT1, p53, and p21, which play significant roles in senescent cells. The gene expression after 3 days is downregulated at all concentrations, which does not provide any indication of senescent cells.

3.1.3. Doxorubicin

3.1.3.1. Long-term titration assay with Doxorubicin

3.1.3.1.1. qPCR

3.1.3.1.1.1. Condrocytes-Doxorubicin

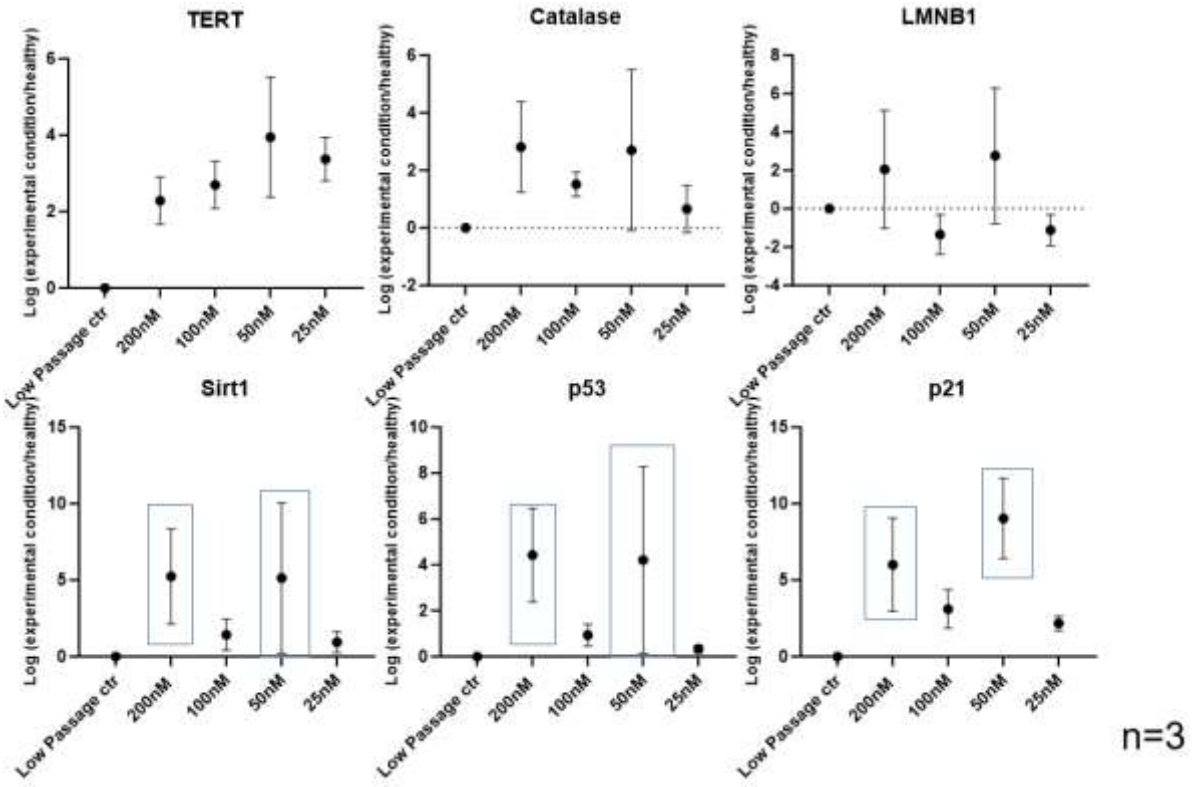

Figure 16 Scatterplots: PCR long-term titration assay with Doxorubicin, Chondrocytes; no statistically significant results

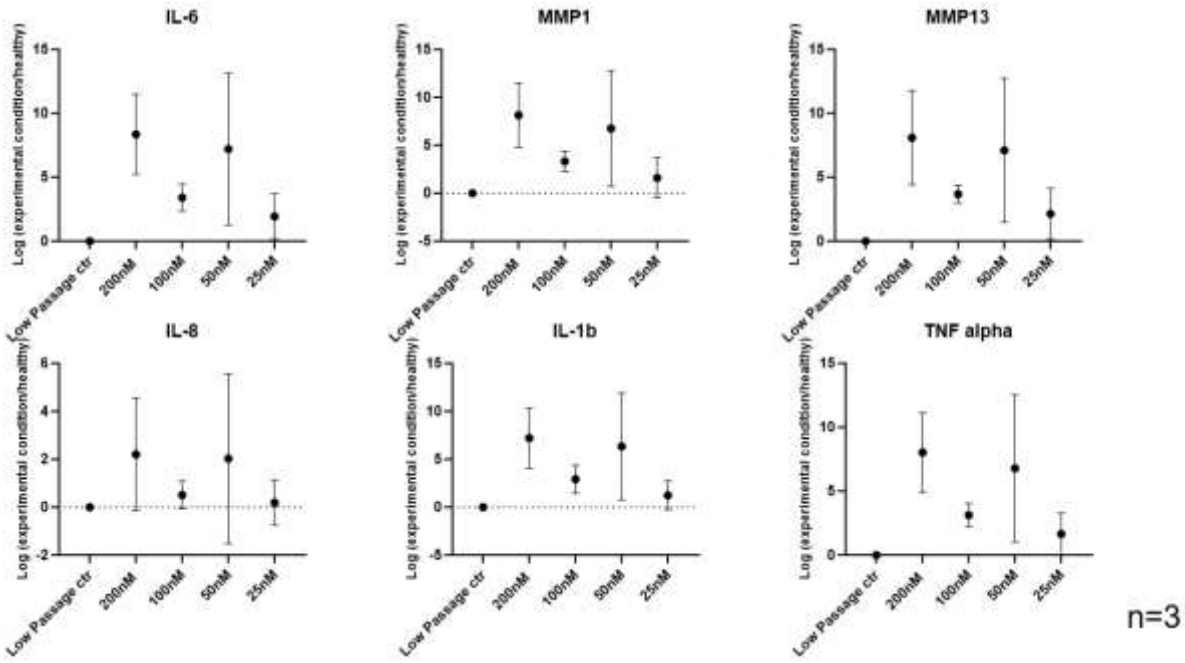

Figure 17 Scatterplots: qPCR long-term titration assay with Doxorubicin, Chondrocytes; no statistically significant results

These graphs (figure 16 and 17) depict the expression of various senescence-associated genes in chondrocytes relative to the concentrations (200 nM, 100 nM, 50 nM, and 25 nM) of Doxorubicin with which these chondrocytes were treated for 6 days. Among all the genes, the highest upregulation was observed at the concentration of 200 nM. At the concentration of 100 nM, the gene expression decreased for all genes, but it increased again at a concentration of 200 nM. The concentration of 25 nM had only a minimal impact on the expression of the p53 gene, with a very slight upregulation of the gene noticeable. P35 is one of the most important proteins that induce cells into senescence, hence the concentration of 25 nM can be ruled out if searching for a concentration of Doxorubicin that induces cells into senescence.

3.1.3.1.1.2. Synoviocytes-Doxorubicin

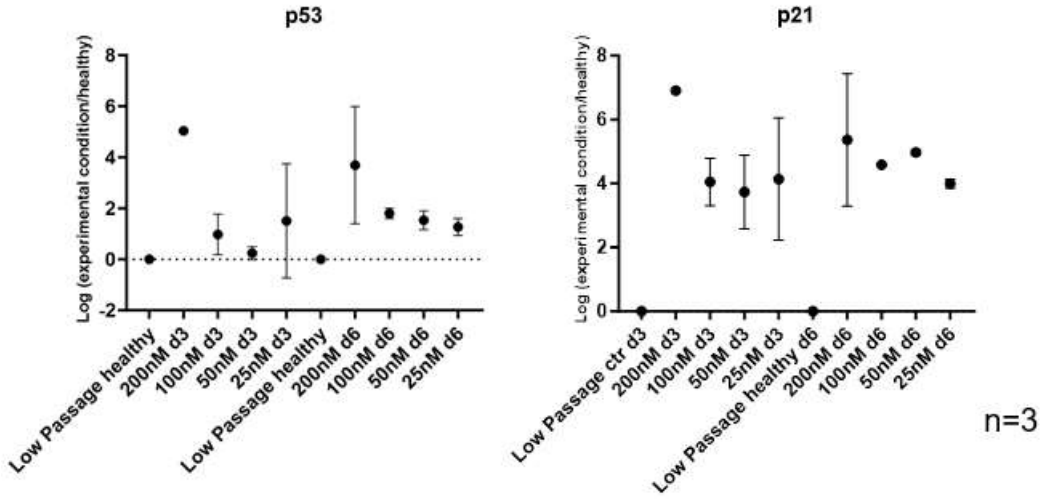

Figure 18 Scatterplots: qPCR long-term titration assay with Doxorubicin, Synoviocytes; no statistically significant results

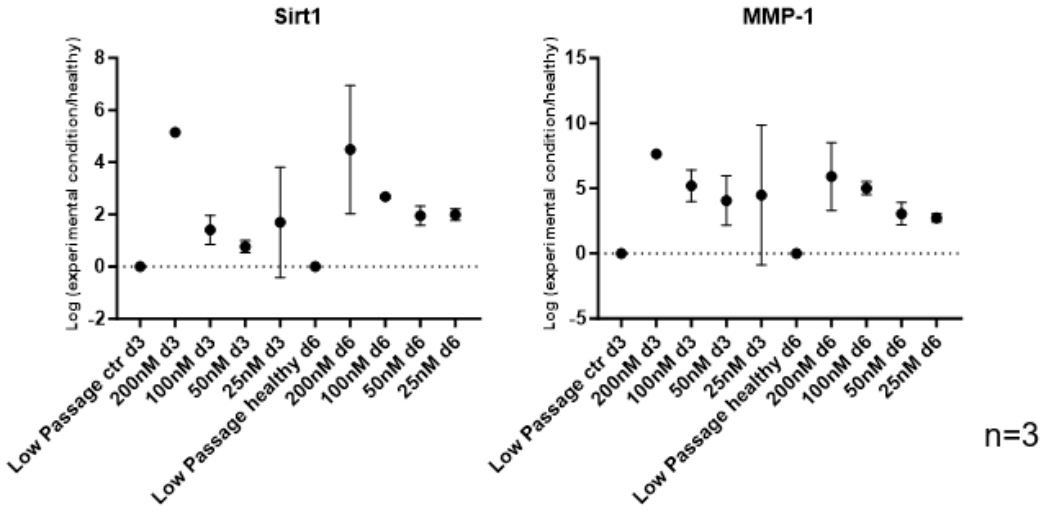

Figure 19 Scatterplots: qPCR long-term titration assay with Doxorubicin, Synoviocytes; no statistically significant results

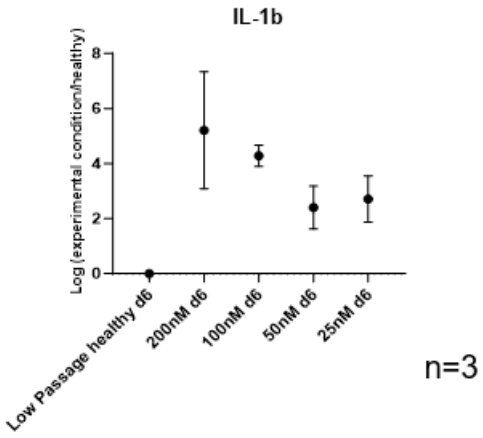

Figure 20 Scatterplots: qPCR long-term titration assay with Doxorubicin, Synoviocytes; no statistically significant results

These graphics (figure 18, 19 and 20) illustrate the expression of senescence-associated genes in synoviocytes in relation to different concentrations (200 nM, 100 nM, 50 nM, and 25 nM) of Doxorubicin, with which the synoviocytes were treated for 6 days, followed by being kept in healthy medium. A qPCR was conducted after 3 days and another after 6 days of being in the healthy medium. When comparing the gene expressions of all genes, it can be observed that both at Day 3 and Day 6, the gene expressions of all genes are most upregulated at a concentration of 200 nM Doxorubicin. Notably, it is observed that p53 is expressed at lower levels in all concentrations compared to p21. (Figure 18) This is surprising since both genes are equally required to produce proteins for senescent cells.

3.1.3.1.2. Cell viability assay (MTT) – Chondrocytes with Doxorubicin

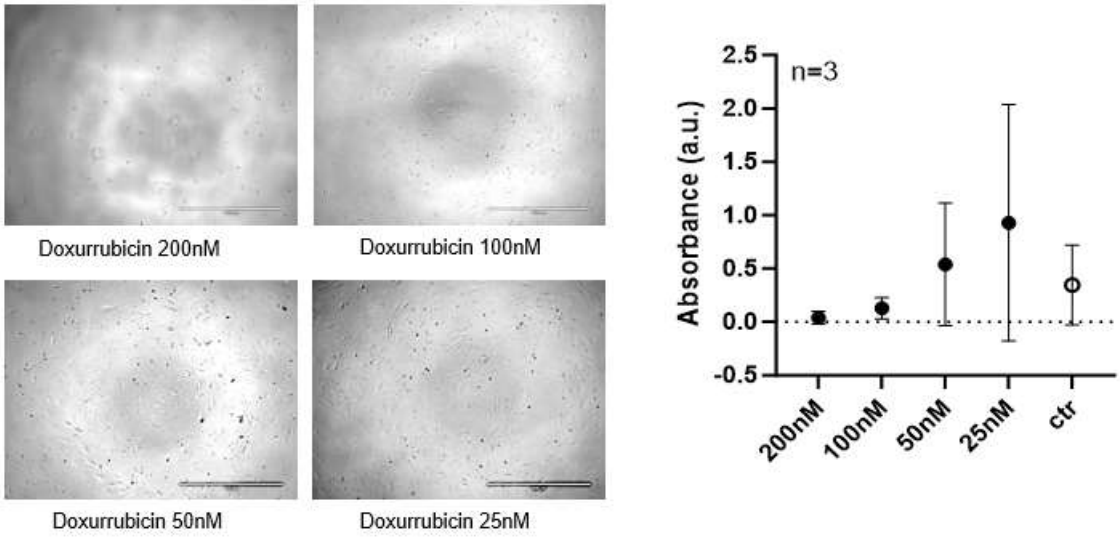

Figure 21 Scatterplots: MTT long-term titration assay with Doxorubicin; Chondrocytes; no statistically significant results

This experiment demonstrates the measurement of optical density at 490 nm of the formed formazan from MTT by chondrocytes in relation to the various concentrations (200 nM, 100 nM, 50 nM, and 25 nM) of Doxorubicin, in which the chondrocytes remained for 6 days and after that for more 6 days in healthy medium. A clear decrease in absorbance, indicating cell viability, is observed with increasing concentration. At concentrations of 200 nM and 100 nM, most cells are dead, the absorbance is near 0, which indicates that the concentration of 200 nM and 100 nM is clearly toxic for the cells. This can also be visually confirmed through images taken under the microscope. At a concentration of 25 nM, the absorbance is higher than in the control group that was not treated with Doxorubicin, indicating increased cell viability. When comparing the 25 nM concentration to the 50 nM concentration, a decrease in absorbance can be observed, which suggests growth arrest and potentially indicates that chondrocytes enter senescence at a concentration of 50 nM Doxorubicin.

3.1.4. Comparison High passaging - Dexamethasone – Doxorubicin

3.1.4.1. Comparison of Chondrocytes exposed to Dexamethasone and Doxorubicin

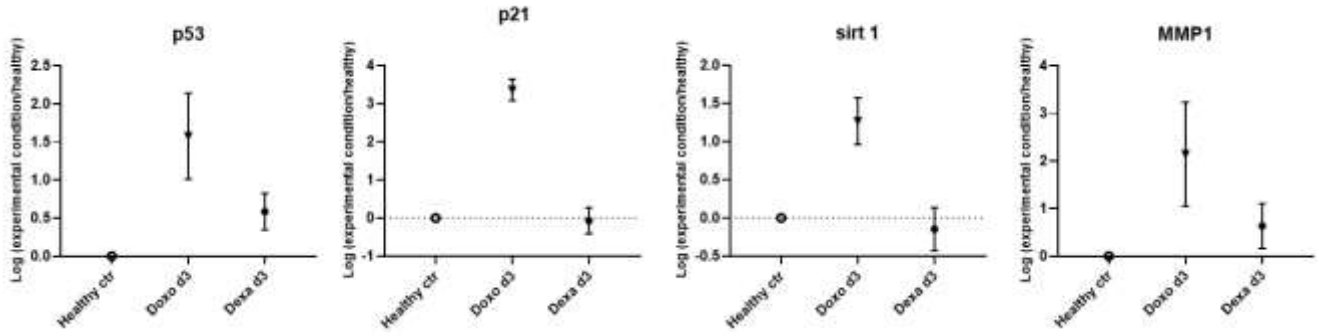

Figure 22 Comparison Chondrocytes Dexamethasone and Doxorubicin Day 3; no statistically significant results

Figure 22 depicts a direct comparison of the gene expressions of p53, p21, SIRT 1, and MMP1 in chondrocytes treated for three days with either the optimal concentration (determined through the long and short-term assays) of Doxorubicin or Dexamethasone. For all four, it can be observed that the treatment with Doxorubicin exhibits higher gene expression of the senescence marker genes after three days compared to the treatment with Dexamethasone.

3.1.4.2. Comparsion of Synoviocytes exposed to Dexamethasone and Doxorubicin

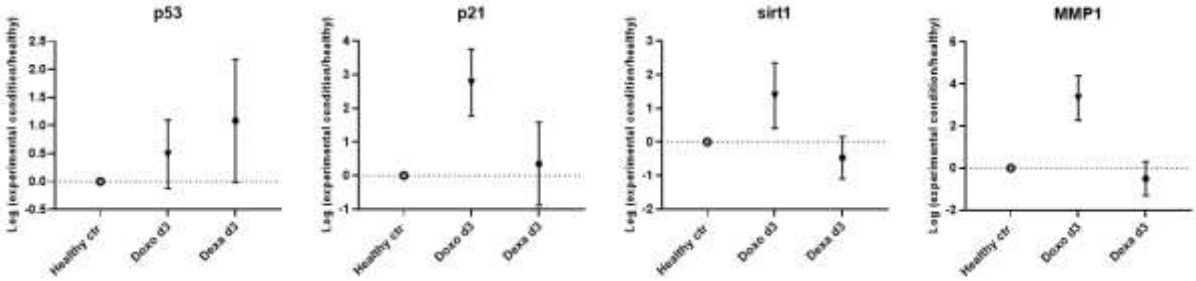

Figure 23 Comparison Synoviocytes Dexamethasone and Doxorubicin Day 3; no statistically significant results

In Figure 23, the same comparison as in Figure 22 was conducted, but with synoviocytes using the same set of genes. Similar trends are observed in the gene expressions of p21, SIRT1, and MMP1 as seen in chondrocytes; Doxorubicin exhibits higher gene expression than

Dexamethasone after three days. However, for p53, gene expression was higher in cells exposed to Dexamethasone than Doxorubicin after 3 days.

In summary, the results indicate that senescence induction can be achieved using Dexamethasone, Doxorubicin, and high passage techniques (confirmed only by cell cycle arrest – proliferation assay).

Cells in passages 49 and higher do not survive freezing post passage 49 for chondrocytes, but cells from passage 31 showed proliferation 6 days after thawing. The proliferation test indicates that chondrocytes exhibit decreased proliferation after 35 passages.

Dexamethasone is recommended at a concentration of 1 μM for chondrocytes and 5 μM for synoviocytes, with both cell types requiring 6 days of incubation. When using Doxorubicin for senescence induction, a concentration of 50 nM is suitable for both chondrocytes and synoviocytes, as higher concentrations exhibit cytotoxic effects.

For future experiments, Dexamethasone appears to be the most practical choice, as it was found which the appropriate concentration and incubation duration is but is also non-cytotoxic compared to Doxorubicin. In contrast to high passaging, the Dexamethasone method is more efficient in terms of time and cost considerations.

4. Discussion

Osteoarthritis, a degenerative joint disease, is characterized by the presence of senescent cells, among other factors (58). In the joint area, chondrocytes and synoviocytes are the predominant cell types, and these cells are primarily responsible for the chronic progression of osteoarthritis with senescence playing an important role in the pathogenesis of OA (19). It is believed that due to chronic inflammation caused by osteoarthritis, which can occur for various reasons such as genetic factors or joint injuries, the cells are no longer able to maintain their homeostasis (59). This results in cellular stress, which can lead to DNA damage and senescence (60). Once cells enter senescence, they remain in a state of growth arrest for an indefinite period (23). Senescent cells produce senescence-associated secretory phenotype (SASP) factors. SASPs are responsible for the release of proinflammatory cytokines such as IL-6 or IL-8, which promote cartilage degeneration (30). This further contributes to more chondrocytes and synoviocytes entering a senescent state, as the cells around the lesion experience increased stress (4). To interrupt and halt this cycle, understanding the characteristics of senescent chondrocytes and synoviocytes is essential.

Various protocols involving different drugs have been developed to induce senescence in vitro. The aim of these studies is to establish standardization for generating in vitro senescent chondrocytes and synoviocytes. This standardization would facilitate future research efforts to discover treatments that can reverse the senescent state in these cells and, consequently, find an effective treatment for osteoarthritis, a condition that currently lacks a proper therapeutic solution. In this study, Dexamethasone and Doxorubicin were used at different concentrations to induce chemically induced senescence. Additionally, chondrocytes that had undergone replicative senescence due to high passaging were examined concerning their proliferation and their behavior after freezing and subsequent thawing.

The seeding test revealed that after 35 passages, cell proliferation decreases rather than increases. However, this test alone cannot determine whether the chondrocytes have entered the senescence state. It can be concluded that cells after 5 passages are definitely not in a senescence state, as they exhibit proliferation, whereas senescent cells are known not to proliferate. (61) It was not surprising to observe that the high-passage chondrocytes displayed a decrease in proliferation. A study by Yang titled 'Changes in phenotype and differentiation potential of human mesenchymal stem cells aging in vitro' investigated mesenchymal stem cells up to passage 8 and noted a decline in proliferation at higher passages (62). This observation aligns with our findings that high-passage chondrocytes exhibit reduced

proliferation. Interestingly, Yang et al. also reported phenotypic changes in cells, a phenomenon we also observed in our high-passage chondrocytes.

Notably, Yang's study revealed that senescence occurred in the early passages due to genetic instability. This suggests that chondrocytes might enter senescence before reaching passage 35, where we typically observe morphological changes and a significant decrease in proliferation. However, it is important to note that Yang's study did not provide details on how senescent cells within the population were confirmed. Thus, while the early onset of senescence is intriguing, further research is needed to confirm and characterize this phenomenon in chondrocytes. To ascertain this, future studies should include a proliferation assay to pinpoint the passage at which cells truly transition into senescence.

It can be concluded that cells after 5 passages are definitely not in a senescence state, as they exhibit proliferation, whereas senescent cells are known not to proliferate (61).

The freezing and thawing test demonstrated that chondrocytes that have undergone 49 passages do not survive the freeze-thaw process. On the other hand, cells from passage 31 can be successfully used after thawing. Cells from passage 49 are in a senescent state, they don’t show any sign of prolieferation; however, they are not practical for in vitro laboratory work due to their inability to withstand freezing, which is a useful preservation method for cell cultures. While cells from passage 31 did survive thawing, it's unlikely that they are in a senescent state, as they exhibited proliferation after thawing. Kim et al. conducted a study on cryopreservation of human ovarian tissue and observed telomere length shortening along with alterations in senescence pathway markers. They postulated that these results were primarily a consequence of DNA damage during the freezing and thawing process rather than an acceleration of cellular senescence (63). Similarly, Honda et al. demonstrated that freezing and thawing retinal pigment epithelial cells resulted in accelerated telomere shortening, compromised proliferation, and DNA breaks (64). The authors suggested that the cryopreservation process itself induced senescence. Another study indicated that cryopreservation of cancer stem cells led to senescence, evidenced by an increase in senescence-associated beta-galactosidase activity (65).

For future studies, it is advisable to complement the freezing and thawing test with a beta-galactosidase assay to confirm whether the cells enter senescence after thawing. It is intriguing that the cells from passage 49 did not survive the process, as previous studies have suggested that freezing cells could promote senescence. However, it's possible that different freezing techniques may yield varying outcomes.

In upcoming research, it would be valuable to explore the senescence potential of chondrocytes at lower passages after freezing and thawing, coupled with a beta-galactosidase test. This approach could shed light on whether chondrocytes subjected to freezing and thawing indeed promote senescence. Additionally, a comparison of the number of chondrocytes in senescence before and after freezing and thawing for passage 31, which was used in this study, could provide valuable insights into senescence dynamics.

Senescent cells typically do not exhibit this level of proliferation and are usually in a state of growth arrest.
In contrast to chemically induced senescence, high passaging (replicative senescence) is more time-consuming. The cells halt their cell cycle in the G1 phase, not in the G2/M phase as observed in chemically induced senescence. During replicative senescence, telomere shortening occurs, while in Doxorubicin-induced senescence, the term "telomere dysfunction" is more commonly used (66). Replicative senescence and chemical-induced senescence differ in the aspects mentioned above and more.

Dexamethasone displayed no toxic effects on the cells at any of the four concentrations (20 µM, 10 µM, 5 µM, and 1 µM), as confirmed by the MTT assay conducted with chondrocytes, reflecting their vitality. All concentrations of Dexamethasone exhibited upregulation of senescence-associated genes in chondrocytes. A slight tendency was observed that 1 µM upregulated the gene expression for senescence markers like p21 and p53 and SASP markers slightly more than other concentrations. This trend was confirmed through the 3-days and 6-days assays, which clearly indicated that all senescence-associated genes in chondrocytes were most upregulated at a concentration of 1 µM at day 6. For synoviocytes, a concentration of 5 µM Dexamethasone was required. It is still unclear why two different concentrations for chondrocytes and synoviocytes are needed to induce senescence, further studies are required to elucidate the underlying mechanisms.
Subsequently, the question arose regarding the optimal incubation duration to achieve the desired effects of Dexamethasone. A short-term assay with chondrocytes revealed that an incubation period of at least 72 hours was necessary to achieve upregulation of senescence-associated gene expression. Interestingly, in the 3-days and 6-days assays, gene expressions for all concentrations were downregulated after 3 days of incubation. Clearly, by day 6, senescence-associated gene expressions in both chondrocytes and synoviocytes were

upregulated, confirming that a minimum 6-day incubation with Dexamethasone with a boost of Dexamethasone on day 3 induces senescence in both cell types.

At a concentration of 200 nM, Doxorubicin demonstrated the highest expression of senescence-associated genes in both chondrocytes and synoviocytes. Wahlmueller et al. conducted a study on the induction of senescence in adipose-derived stromal/stem cells using a 200 nM Doxorubicin treatment, which they found to be the most efficient method (67). Their study involved a treatment duration of 6 days. Interestingly, they observed that at concentrations of 300 and 400 nM, there was a decrease in cell count. This finding aligns with our own study and underscores the critical role of Doxorubicin dosage in determining whether cells enter senescence or undergo apoptosis.
These results from Wahlmueller et al. corroborate our observations, highlighting the significance of selecting the appropriate Doxorubicin concentration for senescence induction. Together with our findings, this adds weight to the notion that Doxorubicin concentration is a key factor in regulating cell fate, be it senescence or apoptosis.
However, the MTT assay performed with chondrocytes indicated that concentrations of 200 nM and 100 nM were toxic to the cells, leading to cell death (55). To prevent this, an optimal concentration of 50 nM was determined for inducing senescence with Doxorubicin in both cell types, as this concentration upregulated gene expression and allowed cell survival. It appears that the optimal Doxorubicin dosage may vary depending on the cell type, suggesting that a nuanced approach is required when selecting the appropriate concentration. Fortunately, in our study, we identified a Doxorubicin dosage that effectively induced senescence in both chondrocytes and synoviocytes. This underscores the need for tailored approaches when working with different cell types, as what works for one may not necessarily be optimal for another.

The results of our study are in alignment with previous publications demonstrating that Dexamethasone's significant downregulation of gene expression in chondrocytes only occurred with an incubation period shorter than three days (51), while an incubation period of 7 days and logner did not result in further increases in sensescent gene expression in tenocytes (68). Similarly, in out study both 24-hour and 48-hour incubations proved insufficient to induce senescence.
After identifying the ideal timing and concentration for the application of Dexamethasone and Doxorubicin for both chondrocytes and synoviocytes, a comparison between Dexamethasone

and Doxorubicin treated cells was pursued. No relevant literature was found on this comparison. Chondrocytes and synoviocytes were treated with the optimal concentration (determined through the long and short-term assays) of Dexamethasone or Doxorubicin, and compared after a 3-day treatment. Overall, higher gene expression of the senescence marker genes p53, p21, SIRT and MMP1 was observed in both cell types treated with Doxorubicin. It was noteworthy that only in synoviocytes, the gene expression of p53 was higher with Dexamethasone than with Doxorubicin treatment. Despite the result suggesting that Doxorubicin appears to have a stronger senescence inducing effect on both cell types, it may not be useful for research in the field of senescence and osteoarthritis due to its known cytotoxic nature, which was also observed in this study.

Furthermore, it should be noted that qPCR only enables the detection of gene expressions, and whether senescence-associated genes indeed translate into proteins cannot be concluded from this study. Thus, future work should involve conducting a beta-galactosidase (beta-gal) assay. Additionally, supernatants of the samples could be collected and further analyzed to gain insight into the cytotome and to examine the chemotaxis contained within it. This would provide conclusions about the proteins involved.

Additionally, it must be mentioned that in vivo, replicative senescence is the predominant form of senescence (69). In vitro, chemical-induced senescence appears advantageous due to its efficiency. In comparaision in vitro high passaging is very time consuming. However, it's important to remember that in vitro conditions may not necessarily mirror the in vivo conditions in the joint during osteoarthritis (66). This should be taken into consideration for further experiments involving chondrocytes and synoviocytes treated with Dexamethasone, Doxurubicine or high passaging. The aim is to find a treatment for reversing senescence and treating osteoarthritis, but the context of in vitro-created cell conditions should be kept in mind.

Conclusion

The conducted tests provide a basis for standardizing future work involving chondrocytes and synoviocytes that are intended to be in a senescent state. This standardization can expedite and simplify future studies aimed at finding treatments to reverse senescence. For inducing chemical senescence in chondrocytes, the recommended approach is to use Dexamethasone at a concentration of 1 μM and an incubation duration of 6 days. In the case of synoviocytes, the suitable concentration of Dexamethasone is 5 μM, and the optimal incubation duration is 6 days. Alternatively, Doxorubicin can be used a concentration of 50 nM to induce senescence in chondrocytes and synoviocytes; however, it is cytotoxic at higher concentrations.

Acknowledgement

A special thank you goes to my supervisor, Priv.-Doz. Dr.med.vet. Iris Gerner, PhD., for her constant understanding and professionalism in addressing my questions and guiding me in the right direction.

A significant contribution was also made by Karyna Tarasova, PhD student, who always had an open ear for my concerns and patiently explained every question, even if I asked it twice.

I would like to express my gratitude to Belen Arteaga, PhD student and Sinan Gültekin, PhD. as well, for their continuous assistance in answering my queries.

A big thanks goes to the entire VETERM team, who welcomed me so warmly during my time in the lab.

Special mention to Jim Knopf, who made my time at VETERM very enjoyable.

5. References

1. Salomon F-V, Geyer H, Gille U, editors. Anatomie für die Tiermedizin. 4. aktualisierte Auflage. Stuttgart: Thieme; 2020.

2. McIlwraith CW, Kawcak CE, Frisbie DD, van Weeren R, editors. Joint Disease in the Horse (Second Edition). Second edition. St. Louis, Missouri: W B Saunders Company; 2016. Available from: URL: http://www.sciencedirect.com/science/book/9781455759699.

3. Aurich C. Anatomie der Haustiere: Lehrbuch und Farbatlas für Studium und Praxis. 7., aktualisierte und erweiterte Auflage. Stuttgart: Georg Thieme Verlag; 2019.

4. Rim YA, Nam Y, Ju JH. The Role of Chondrocyte Hypertrophy and Senescence in Osteoarthritis Initiation and Progression. Int J Mol Sci 2020; 21(7).

5. McIlwraith CW, Fortier LA, Frisbie DD, Nixon AJ. Equine Models of Articular Cartilage Repair. Cartilage 2011; 2(4):317–26.

6. Zhang M, Theleman JL, Lygrisse KA, Wang J. Epigenetic Mechanisms Underlying the Aging of Articular Cartilage and Osteoarthritis. Gerontology 2019; 65(4):387–96.

7. Goodrich LR, Nixon AJ. Medical treatment of osteoarthritis in the horse - a review. Vet J 2006; 171(1):51–69.

8. Ortved KF, Nixon AJ. Cell-based cartilage repair strategies in the horse. Vet J 2016; 208:1–12.

9. Decker RS, Koyama E, Pacifici M. Articular Cartilage: Structural and Developmental Intricacies and Questions. Curr Osteoporos Rep 2015; 13(6):407–14.

10. Mobasheri A, Matta C, Zákány R, Musumeci G. Chondrosenescence: definition, hallmarks and potential role in the pathogenesis of osteoarthritis. Maturitas 2015; 80(3):237–44.

11. Aigner T, Söder S, Gebhard PM, McAlinden A, Haag J. Mechanisms of disease: role of chondrocytes in the pathogenesis of osteoarthritis--structure, chaos and senescence. Nat Clin Pract Rheumatol 2007; 3(7):391–9.

12. Zheng L, Zhang Z, Sheng P, Mobasheri A. The role of metabolism in chondrocyte dysfunction and the progression of osteoarthritis. Ageing Res Rev 2021; 66:101249.

13. Salomon F-V, Geyer H, editors. Atlas der angewandten Anatomie der Haustiere. 4. Auflage. Stuttgart: Enke Verlag in MVS Medizinverlage Stuttgart GmbH & Co KG; 2014.

14. Iwanaga T, Shikichi M, Kitamura H, Yanase H, Nozawa-Inoue K. Morphology and functional roles of synoviocytes in the joint. Arch Histol Cytol 2000; 63(1):17–31.

15. Guilak F. Biomechanical factors in osteoarthritis. Best Pract Res Clin Rheumatol 2011; 25(6):815–23.

16. Sanchez-Lopez E, Coras R, Torres A, Lane NE, Guma M. Synovial inflammation in osteoarthritis progression. Nat Rev Rheumatol 2022; 18(5):258–75.

17. Orlowsky EW, Kraus VB. The role of innate immunity in osteoarthritis: when our first line of defense goes on the offensive. J Rheumatol 2015; 42(3):363–71.

18. Liu J, Wang L, Wang Z, Liu J-P. Roles of Telomere Biology in Cell Senescence, Replicative and Chronological Ageing. Cells 2019; 8(1).

19. Liu Y, Zhang Z, Li T, Xu H, Zhang H. Senescence in osteoarthritis: from mechanism to potential treatment. Arthritis Res Ther 2022; 24(1):174.

20. Fisch KM, Gamini R, Alvarez-Garcia O, Akagi R, Saito M, Muramatsu Y et al. Identification of transcription factors responsible for dysregulated networks in human osteoarthritis cartilage by global gene expression analysis. Osteoarthritis Cartilage 2018; 26(11):1531–8.

21. Hernandez-Segura A, Nehme J, Demaria M. Hallmarks of Cellular Senescence. Trends Cell Biol 2018; 28(6):436–53.

22. Kowald A, Passos JF, Kirkwood TBL. On the evolution of cellular senescence. Aging Cell 2020; 19(12):e13270.

23. Roger L, Tomas F, Gire V. Mechanisms and Regulation of Cellular Senescence. Int J Mol Sci 2021; 22(23).

24. Campisi J. Aging, cellular senescence, and cancer. Annu Rev Physiol 2013; 75:685–705.

25. Bu H, Wedel S, Cavinato M, Jansen-Dürr P. MicroRNA Regulation of Oxidative Stress-Induced Cellular Senescence. Oxid Med Cell Longev 2017; 2017:2398696.

26. Magalhães JP de, Passos JF. Stress, cell senescence and organismal ageing. Mech Ageing Dev 2018; 170:2–9.

27. Chandeck C, Mooi WJ. Oncogene-induced cellular senescence. Adv Anat Pathol 2010; 17(1):42–8.

28. Liu X-L, Ding J, Meng L-H. Oncogene-induced senescence: a double edged sword in cancer. Acta Pharmacol Sin 2018; 39(10):1553–8.

29. McHugh D, Gil J. Senescence and aging: Causes, consequences, and therapeutic avenues. J Cell Biol 2018; 217(1):65–77.

30. Lopes-Paciencia S, Saint-Germain E, Rowell M-C, Ruiz AF, Kalegari P, Ferbeyre G. The senescence-associated secretory phenotype and its regulation. Cytokine 2019; 117:15–22.

31. Choi M-C, Jo J, Park J, Kang HK, Park Y. NF-κB Signaling Pathways in Osteoarthritic Cartilage Destruction. Cells 2019; 8(7).

32. Jackson SP, Bartek J. The DNA-damage response in human biology and disease. Nature 2009; 461(7267):1071–8.

33. Issa RI, Griffin TM. Pathobiology of obesity and osteoarthritis: integrating biomechanics and inflammation. Pathobiol Aging Age Relat Dis 2012; 2(2012).

34. Roy N, Bagchi S, Raychaudhuri P. Damaged DNA binding protein 2 in reactive oxygen species (ROS) regulation and premature senescence. Int J Mol Sci 2012; 13(9):11012–26.

35. Vinatier C, Domínguez E, Guicheux J, Caramés B. Role of the Inflammation-Autophagy-Senescence Integrative Network in Osteoarthritis. Front Physiol 2018; 9:706.

36. Glorieux C, Calderon PB. Catalase, a remarkable enzyme: targeting the oldest antioxidant enzyme to find a new cancer treatment approach. Biol Chem 2017; 398(10):1095–108.

37. Terlecky SR, Koepke JI, Walton PA. Peroxisomes and aging. Biochim Biophys Acta 2006; 1763(12):1749–54.

38. Nandi A, Yan L-J, Jana CK, Das N. Role of Catalase in Oxidative Stress- and Age-Associated Degenerative Diseases. Oxid Med Cell Longev 2019; 2019:9613090.

39. Calcinotto A, Kohli J, Zagato E, Pellegrini L, Demaria M, Alimonti A. Cellular Senescence: Aging, Cancer, and Injury. Physiol Rev 2019; 99(2):1047–78.

40. Toh WS, Brittberg M, Farr J, Foldager CB, Gomoll AH, Hui JHP et al. Cellular senescence in aging and osteoarthritis. Acta Orthop 2016; 87(sup363):6–14.

41. Coryell PR, Diekman BO, Loeser RF. Mechanisms and therapeutic implications of cellular senescence in osteoarthritis. Nat Rev Rheumatol 2021; 17(1):47–57.

42. Rufini A, Tucci P, Celardo I, Melino G. Senescence and aging: the critical roles of p53. Oncogene 2013; 32(43):5129–43.

43. Sheekey E, Narita M. p53 in senescence - it's a marathon, not a sprint. FEBS J 2023; 290(5):1212–20.

44. Pawge G, Khatik GL. p53 regulated senescence mechanism and role of its modulators in age-related disorders. Biochem Pharmacol 2021; 190:114651.

45. Mijit M, Caracciolo V, Melillo A, Amicarelli F, Giordano A. Role of p53 in the Regulation of Cellular Senescence. Biomolecules 2020; 10(3).

46. Ji M-L, Jiang H, Li Z, Geng R, Hu JZ, Lin YC et al. Sirt6 attenuates chondrocyte senescence and osteoarthritis progression. Nat Commun 2022; 13(1):7658.

47. Brazvan B, Ebrahimi-Kalan A, Velaei K, Mehdipour A, Aliyari Serej Z, Ebrahimi A et al. Telomerase activity and telomere on stem progeny senescence. Biomed Pharmacother 2018; 102:9–17.

48. Yuan X, Larsson C, Xu D. Mechanisms underlying the activation of TERT transcription and telomerase activity in human cancer: old actors and new players. Oncogene 2019; 38(34):6172–83.

49. Ling X, Yang W, Zou P, Zhang G, Wang Z, Zhang X et al. TERT regulates telomere-related senescence and apoptosis through DNA damage response in male germ cells exposed to BPDE in vitro and to BaP in vivo. Environ Pollut 2018; 235:836–49.

50. Ge H, Ke J, Xu N, Li H, Gong J, Li X et al. Dexamethasone alleviates pemetrexed-induced senescence in Non-Small-Cell Lung Cancer. Food Chem Toxicol 2018; 119:86–97.

51. Xue E, Zhang Y, Song B, Xiao J, Shi Z. Effect of autophagy induced by dexamethasone on senescence in chondrocytes. Mol Med Rep 2016; 14(4):3037–44.

52. Parajuli P, Rosati R, Mamdani H, Wright RE, Hussain Z, Naeem A et al. Senescence-associated secretory proteins induced in lung adenocarcinoma by extended treatment with dexamethasone enhance migration and activation of lymphocytes. Cancer Immunol Immunother 2023; 72(5):1273–84.

53. Carvalho C, Santos RX, Cardoso S, Correia S, Oliveira PJ, Santos MS et al. Doxorubicin: the good, the bad and the ugly effect. Curr Med Chem 2009; 16(25):3267–85.

54. Karabicici M, Alptekin S, Fırtına Karagonlar Z, Erdal E. Doxorubicin-induced senescence promotes stemness and tumorigenicity in EpCAM-/CD133- nonstem cell population in hepatocellular carcinoma cell line, HuH-7. Mol Oncol 2021; 15(8):2185–202.

55. Wu C, Luo J, Liu Y, Fan J, Shang X, Liu R et al. Doxorubicin suppresses chondrocyte differentiation by stimulating ROS production. Eur J Pharm Sci 2021; 167:106013.

56. Armstrong J, Dass CR. Doxorubicin Action on Mitochondria: Relevance to Osteosarcoma Therapy? Curr Drug Targets 2018; 19(5):432–8.

57. Kciuk M, Gielecińska A, Mujwar S, Kołat D, Kałuzińska-Kołat Ż, Celik I et al. Doxorubicin-An Agent with Multiple Mechanisms of Anticancer Activity. Cells 2023; 12(4).

58. McCulloch K, Litherland GJ, Rai TS. Cellular senescence in osteoarthritis pathology. Aging Cell 2017; 16(2):210–8.

59. Regulski MJ. Cellular Senescence: What, Why, and How. Wounds 2017; 29(6):168–74.

60. Lepetsos P, Papavassiliou AG. ROS/oxidative stress signaling in osteoarthritis. Biochim Biophys Acta 2016; 1862(4):576–91.

61. Alcorta DA, Xiong Y, Phelps D, Hannon G, Beach D, Barrett JC. Involvement of the cyclin-dependent kinase inhibitor p16 (INK4a) in replicative senescence of normal human fibroblasts. Proc Natl Acad Sci U S A 1996; 93(24):13742–7.

62. Yang Y-HK, Ogando CR, Wang See C, Chang T-Y, Barabino GA. Changes in phenotype and differentiation potential of human mesenchymal stem cells aging in vitro. Stem Cell Res Ther 2018; 9(1):131.

63. Kim B, Ryu K-J, Lee S, Kim T. Changes in telomere length and senescence markers during human ovarian tissue cryopreservation. Sci Rep 2021; 11(1):2238.

64. Honda S, Weigel A, Hjelmeland LM, Handa JT. Induction of telomere shortening and replicative senescence by cryopreservation. Biochem Biophys Res Commun 2001; 282(2):493–8.

65. Karimi-Busheri F, Zadorozhny V, Shawler DL, Fakhrai H. The stability of breast cancer progenitor cells during cryopreservation: Maintenance of proliferation, self-renewal, and senescence characteristics. Cryobiology 2010; 60(3):308–14.

66. Bielak-Zmijewska A, Wnuk M, Przybylska D, Grabowska W, Lewinska A, Alster O et al. A comparison of replicative senescence and doxorubicin-induced premature senescence of vascular smooth muscle cells isolated from human aorta. Biogerontology 2014; 15(1):47–64.

67. Wahlmueller M, Narzt M-S, Missfeldt K, Arminger V, Krasensky A, Lämmermann I et al. Establishment of In Vitro Models by Stress-Induced Premature Senescence for Characterizing the Stromal Vascular Niche in Human Adipose Tissue. Life (Basel) 2022; 12(10).

68. Poulsen RC, Watts AC, Murphy RJ, Snelling SJ, Carr AJ, Hulley PA. Glucocorticoids induce senescence in primary human tenocytes by inhibition of sirtuin 1 and activation of the p53/p21 pathway: in vivo and in vitro evidence. Ann Rheum Dis 2014; 73(7):1405–13.

69. Halliwell B. Cell culture, oxidative stress, and antioxidants: avoiding pitfalls. Biomed J 2014; 37(3):99–105. Available from: URL: https://pubmed.ncbi.nlm.nih.gov/24923566/.

5.1. Figures

5.2. Tables

5.3. Abbkürzungsverzeichnis

°C - Degree Celsius
µl - Microliter
µM - Micromolar
APC/C – Anaphase-promoting complex / cyclosome
ATM - Ataxia Telangiectasia Mutated
C/EBP-β - CCAT/Enhancer Binding Protein
CDK2 - Cyclin-dependent Kinase 2
CDKs - Cyclin-dependent kinases
cm² - Square centimeters
CO_2 - Carbon dioxide
CT - C-terminal
DDR - DNA damage response
DEPC (water) - Diethylpyrocarbonate (water)
DMEM - Dulbecco's Modified Eagle Medium
DNA - Dulbecco's Modified Eagle Medium
ECM - Extracellular matrix
EDTA - Ethylenediaminetetraacetic Acid
FCS - Fetal calf serum
g- Gram
GAPD - Ethylenediaminetetraacetic Acid
IL-1beta - Interleukin-1 beta
IL-6 - Interleukin-6
IL-8 - Interleukin-6
MCPs - Monocyte Chemoattractant Proteins
MIPs - Macrophage Inflammatory Proteins
ml - Milliliters
MMP1 - Matrix Metalloproteinase-1
MMP13 - Matrix Metalloproteinase-13
MMPs - Matrix Metalloproteinases
MTT - 3-(4,5-dimethylthiazol-2-yl)-2,5-diphenyltetrazolium bromide) cytotoxicity assay
NAD+ - Nicotinamide Adenine Dinucleotide (oxidized form)
NF-kB - Nuclear factor ‘kappa-light-chain-enhancer’ of activated B-cells

nM – Nanomolar

NT - N-terminal

OA – Osteoarthritis

OIS - Oncogene-induced Senescence

P – Passage

p16 - Cyclin-dependent Kinase Inhibitor 2A (CDKN2A)

p16INK4a - Cyclin-dependent Kinase Inhibitor 2A (CDKN2A) alternate name

p19ARF - Alternate Reading Frame Protein of the INK4a/ARF Locus

p21 - Cyclin-dependent Kinase Inhibitor 1 (CDKN1A)

p21CIP1 - Cyclin-dependent Kinase Inhibitor 1 (CDKN1A)

p27 - Cyclin-dependent Kinase Inhibitor 1B (CDKN1B)

p53 - Tumor Protein p53

PAI-1 - Plasminogen Activator Inhibitor-1

PBS - Phosphate-buffered saline

pH – Potential of Hydrogen

pRB - Retinoblastoma protein

PS - Penicillin-Streptomycin

qPCR - Quantitative Polymerase Chain Reaction

RNA - Ribonucleic Acid

ROS - Reactive Oxygen Species

RPBI - Ribonucleic Acid

Rpm - Ribonucleic Acid

RS – Replicative Senescence

SASP - Senescence-Associated Secretory Phenotype factors

SA-β-gal - Senescence-associated β-galactosidase

SIPS - Stress-induced Premature Senescence

SIRT 1 – Sirtuin 1

T175 - T-flask 175 cm^2

TERT - Telomerase Reverse Transcriptase

TNF alpha - Tumor Necrosis Factor alpha